1995

The design of a continuous-time log-domain adaptive filter using complementary bipolar technology

Luke T. Steigerwald
Lehigh University

AUTHOR:

Steigerwald, Luke T.

TITLE:

The Design of a Continuous-Time Log-Domain Adaptive Filter Using Complementary Bipolar Technology

DATE: May 28, 1995

The Design of a Continuous-time Log-domain Adaptive Filter Using Complementary Bipolar Technology

by

Luke T. Steigerwald

A Thesis
Presented to the Graduate and Research Committee
of Lehigh University
in Candidacy for the Degree of
Master of Science

in
Electrical Engineering

Lehigh University

5/05/95

This thesis is accepted and approved in partial fulfillment of the requirements for the degree of Master of Science.

5/05/95 5/5/95
Date

Thesis Advisor

Chairperson of Department

TABLE OF CONTENTS

LIST OF FIGURES

ABSTRACT

Log-domain filter theory [1] is revisited in this work by initially describing a first order lowpass log filter. A log domain gyrator is presented and is used in the implementation of highpass and notch log filter functions. An adaptive notch log filter is then presented. The filter adapts its resonant frequency to the fundamental frequency of an input sinusoid and provides both notch and bandpass outputs for the detection and enhancement of the input signal. Simulation results are presented for a filter that adapts its resonant frequency to detect and enhance a 6 MHz input sine wave using transistor models from AT&T's CBIC-R 300 MHz complementary bipolar process. In addition, parallel filter sections are used in the design of an adaptive filter that detects and enhances multiple input sinusoids. Given a signal that is the sum of 3 MHz and 2.77 MHz sine waves as its input, this filter is shown in simulation to recover the two independent sine waves, providing notch and bandpass outputs for both.

INTRODUCTION

A new class of filters has been developed which offer advantages over conventional filters[1]. Log-domain, or simply log, filters make use of the logarithmic relationship between voltage and current in bipolar transistors. The main advantages of log filters are that they are useful to very high frequencies with a large dynamic range while utilising relatively few parts. Log filters are implemented using only capacitors, emitter followers, and current sources. There are many applications which require the detection and enhancement of sinusoidal signals corrupted by noise, the most notable being in the fields of communications and radar. Because of the excellent frequency response of log filters, very high frequency sinusoids will be able to be detected and enhanced. Extremely weak sinusoidal signals signals buried in noise will also be able to be detected and enhanced because of the increased dynamic range of log filters.

A first order lowpass log filter will first be discussed. The concept of a log domain gyrator will be introduced that extends the lowpass log filter circuit into a highpass filter realisation. This log domain gyrator will also be used in the design of a composite notch/bandpass log filter which provides both notch and bandpass outputs to an

input sinusoid. This filter forms the basis for the design of an adaptive log filter. The filter adapts its resonant frequency to the frequency of the input sinusoid. The desired response of the filter is to achieve zero AC response at the notch output. The adaptive filter adjusts its parameters until this specification is met. Because the resonant frequency of the bandpass filter is the same as that of the notch filter, an enhanced version of the sinusoid is available at the bandpass output for characterization. An adaptive notch filter that notches two independent input sinusoids is designed by placing an additional notch block in parallel with the existing notch block.

LOG FILTER THEORY

A log filter can be broken up into three stages; the input stage, the log-domain stage, and the output stage. The purpose of the input stage is to take the natural logarithm of the input signal, presumably a current. The log-domain stage achieves the intended filtering process with a log-domain filter. The output stage exponentiates the log signal, thus recovering a linearly filtered version of the input signal.

Figure 1 shows the simplified schematic of a first-order log-domain lowpass filter. The input diode, D, takes the log of I_{in}, the input current. The current source I_{dc} is needed to ensure that the input current remains positive at all times for all possible signal amplitudes. Since the overall transfer function from input to output is linear, this source will merely add DC to the output without affecting the filter response in any way. Q1, I_0, and C comprise the actual log filter. The transistor Q1 together with the current source I_0 can be modelled as a resistor equal to the dynamic impedance of Q1's base emitter diode, r_d, where:

$$r_d = 1/kI_0, \quad k= q/kT = 38.64 \text{ V}. \qquad (1)$$

Thus, Q1, I_0, and C implement a lowpass filter with cutoff frequency w_c:

$$w_c = 1/RC = 1/(1/kI_0)C = kI_0/C. \qquad (2)$$

By varying the magnitude of I_0, the filter can be electronically tuned.

A state space approach was used to originally design this log filter [1]. The following state space description may be used:

$$dX/dt = -w_0X + w_0U \; ; \; Y = X, \qquad (3)$$

where U is the input, Y is the output, and X is the state variable. If U and X are mapped as follows:

$$U = e^{kVin} \qquad (4)$$

$$X = e^{kV1},$$

and the state equation is scaled by Ce^{-kV1}/k, where C is positive and real, the following equation results:

$$CdV_1/dt = -I_0 + I_0e^{k(Vin - V1)};$$

$$Y = e^{kV1}, \qquad (5)$$

where $I_0 = w_0C/k$.

By referring to Fig. 1, it is seen that this equation is a node equation at node 1, which states that the current through the capacitor C is equal to the sum of I_0 and the current flowing in the base-emitter diode of Q1.

Complementary bipolar devices were used to implement the design of Figure 1. This removes the requirement that NPN and PNP transistors match. Also, every composite diode junction formed by an NPN and a PNP transistor can be thought of as a single device. This device follows the diode law:

$$I = I_0 e^{k'V}; \qquad (6)$$

except that $k'=k/2=q/2kT$. From here on this quantity will be referred to as merely k.

The first order lowpass log filter is shown in Fig. 2. Q1 and Q2 comprise the input logging diode, Q4 and Q5 comprise the emitter follower transistor, Q6 and Q7 comprise the level shift V_d, and Q9 and Q10 comprise the output exponentiating transistor Q2 from Fig. 1. Q3, Q8, and Q13 are added to the current mirror configurations to increase the achievable current gain by a factor of 6. These transistors also reduce errors due to non-zero base currents. Q4 and Q9 are tied to 1.9 V and Q14 is tied to -1.9 V to lessen the effect of the early voltage.

An ideal integrator can be designed if the source I_0 is removed from Fig. 2. Conceptually, this circuit can be thought of as a lowpass filter with a cutoff frequency equal to zero, as seen by setting $I_0 = 0$ in eqn. 2. An additional reference circuit is connected to node 1, as shown in Fig. 3. The reference circuit is needed to balance the currents at node 1 so that an appropriate DC equilibrium exists. This block will be called the null block. It's purpose is to pull I_0 amps from node 1.

The design procedure for realising a second order lowpass log filter starts with the determination of a suitable state-space description. An exponential transformation is then applied to the state equation. The

result is a set of nodal equations which can be implemented by the proper interconnection of transistors. The second order log filter will have two node voltages tying capacitors to ground rather than the one node voltage observed in the first order case. The interested reader is referred to [1] for a complete general design procedure for the creation of log filters. Higher order filters can easily be implemented by cascading first and second order filter sections.

LOG DOMAIN GYRATOR AND ITS USE IN LOG FILTER TOPOLOGIES

In the previous section the use of log filters in first order lowpass filter functions was described. In this section, the use of a log domain gyrator to implement highpass, notch, and bandpass filter functions will be presented.

The extension of the lowpass log filter to other filter implementations is not obvious. A log-domain gyrator will allow an effective inductance to be synthesized from a physical capacitance, thereby creating an effective parallel L,R connection and a highpass filter function.

A linear gyrator may be implemented by connecting a positive transconductance block and a negative transconductance block as shown in Fig. 4. It is seen that:

$$V_2 = I_2 z = G_m V_1 Z \qquad (7)$$

$$-I_1 = -G_m V_2,$$

so that:

$$I_1 = G_m(G_m V_1 Z) = G_m^2 V_1 Z. \qquad (8)$$

Therefore the impedance seen at node 1, Z_{eq}, is:

$$Z_{eq} = V_1/I_1 = V_1/G_m^2 V_1 Z = 1/G_m^2 Z. \qquad (9)$$

By connecting a capacitor from the output of the gyrator to ground an effective inductance can be created. A simplified schematic of a highpass log filter is shown in Fig. 5 [2]. The input of the gyrator is connected to node 1 and capacitor C is connected to the output of the gyrator. As

with the lowpass filter, the voltage at node 1 is level shifted by V_d and exponentiated by Q2 to produce a linear highpass filter function at the output.

A log domain gyrator can be implemented by using current mirrors as the transconductance blocks as shown in Fig. 6. The transconductance G_m is that of a bipolar transistor except that because of the double diode drops, $V_t' = 2V_t$, and

$$G_m = I_0/V_t' = kI_0, \qquad (10)$$

where $k = q/2kT$. The complete schematic for the highpass log filter is shown in Fig. 7. The null block made up of transistors Q21-Q25 is again used to achieve a suitable DC operating point. The current mirror of transistors Q16-Q20 comprises the output exponentiating stage. The base of transistor Q25 is connected to an additional current mirror to balance the DC operating points of the capacitor node voltages. Capacitor C2 is set much greater than C1 so that infinite impedance is reflected over to node 2. The current source I_{06} is set to a value equal to the sum of I_{01} and I_{03} so that it pulls the same amount of current from node 3 as is pulled from node 1, and, by setting I_{dc2} equal to I_{dc1}, this ensures that the voltage at node 3 equals the voltage at node 1. This filter is also electronically tunable, with the cutoff frequency w_c:

$$w_c = R/L = G_m^2R/C = [kI_0]^2R/C = kI_0/C, \qquad (11)$$

since $R = 1/(kI_0)$.

Another look at the configuration in Fig. 6 proves that it does indeed realize a linear highpass response from the input current to the output current. The following equations can be derived:

$$I_0 = I_s e^{k(Vin - V1)} - I_s e^{k[Vc - (Vi - Vd)]} \quad (12)$$

$$I_c = CdV_c/dt = I_s e^{k(V1 + Vd - Vc)} - I_s e^{k[Vdc - (V1 - Vd)]} \quad (13)$$

$$I_{out} = I_s e^{k(V1 + Vd)}. \quad (14)$$

However, it is seen that:

$$V_{in} = (1/k)\ln(I_{in}/I_s) \quad (15)$$

$$V_d = (1/k)\ln(I_0/I_s).$$

Substituting these voltages into the first set of equations yields:

$$I_{in} = I_0 e^{kV1} + I_0 e^{kVc} \quad (16)$$

$$CdV_c/dt = I_0 e^{kV1} - I_0 e^{kVdc} \quad (17)$$

$$I_{out} = I_0 e^{kV1}. \quad (18)$$

Differentiating eqn. 16 yields:

$$dI_{in}/dt = kdV_1/dtI_0 e^{kV1} + kdV_c/dtI_0 e^{kVc} \quad (19)$$

Solving eqn. 17 for dV_c/dt and substituting this into eqn. 19 yields:

$$kdV_1/dtI_0 e^{kV1} + (kI_0^2/C)(e^{kV1} - e^{kVdc}) + dI_{in}/dt \quad (20)$$

If $X = I_0 e^{kV1}$, this simplifies to:

$$dX/dt + w_0 X + w_0 U_{dc} = dI_{in}/dt, \quad (21)$$

where $w_0 = (kI_0/C)$ and $U_{dc} = I_0 e^{kVdc}$. This is the linear differential equation for a highpass filter function, proving that although the log filter processes signals

nonlinearly, the output does provide a linearly filtered version of the input.

The log gyrator used in the highpass design may also be used to implement notch and bandpass filters. In fact, by using two gyrators a filter that has a notch response at one output while having a bandpass response at another output can be designed. By connecting a capacitor to its output, the first gyrator will be used to simulate an inductor as was done in the highpass filter. Another capacitor can be placed in parallel to implement a bandpass filter function. By placing another gyrator in front of this effective parallel L,C impedance, a series L,C connection will be achieved, thus creating a notch response. This notch/bandpass log filter is shown in Fig. 8.

Gyrator 2 transforms C2 into an inductance, which, when placed in parallel with C1, creates a bandpass response at node 2. A level shift and an exponentiator, transistor Q3, recover the linearly filtered bandpass response. Gyrator 1 reflects this parallel L,C combination into a series L,C impedance. This is placed in parallel with a resistor, current source I_0, to form the notch function. V_d and Q2 likewise recover the linear version of this notch response.

The determination of capacitor values C1 and C2 to effect a desired Q is as follows. The Q of the bandpass filter is:

$$Q = 1/R\sqrt{(L/C)}. \qquad (22)$$

From Fig. 7 it is easy to see that gyrator 2 synthesizes an effective inductance L1 from C2;

$$L1 = C2/G_{m2}^2, \qquad (23)$$

where G_{m2} is the transconductance of gyrator 2. Therefore the circuit can be simplified to that of Fig. 9. Gyrator 1 transforms the parallel L1,C1 combination into a series combination. L1 is reflected into C_{eff};

$$C_{eff} = G_{m1}^2 L1 = G_{m1}^2 (C2/G_{m2}^2), \qquad (24)$$

and C1 is reflected into L_{eff};

$$L_{eff} = C1/G_{m1}^2, \qquad (25)$$

where G_{m1} is the transconductance of gyrator 1. Since $R = 1/kI_{01}$;

$$Q = (1/(1/kI_{01}))\sqrt{[(C1/G_{m1}^2)/G_{m1}^2(C2/G_{m2}^2)]}$$
$$= (G_{m2}/(G_{m1}^2/kI_{01}))\sqrt{[C1/C2]}. \qquad (26)$$

If the set currents in gyrator 1 are set equal to the set currents in gyrator 2, and G_m is set equal to kI_0, then Q becomes;

$$Q = (kI_0/(k^2I_0^2/kI_{01}))\sqrt{[C1/C2]}$$
$$= (I_{01}/I_0)\sqrt{[C1/C2]}. \qquad (27)$$

Thus the Q of the filter can be controlled by changing the ratio of the capacitors or by changing the ratio of the resistive current source I_{01} to the set currents, I_0. The complete schematic for this notch/bandpass log filter is shown in Fig. 10. The current mirror comprising transistors Q41-Q45 is again used to balance the DC operating points of the capacitor node voltages.

The filter was simulated with the set currents I_0 as well as the resistive current source I_{01} set to 100 uA. PSpice was the simulation tool used, and ideal transistor models with a β=10000 were used. C1 was chosen to be 250 pF and C2 was chosen to be 10 pF. This achieves a Q equal to 5. The PSpice netlist for this filter is shown in Appendix A. The frequency-response characteristics of the notch output and the bandpass output are shown in Fig. 11. The resonant frequency of the filter is determined by:

$$f_r = (1/2\pi)1/\sqrt{[L_{eff}C_{eff}]} = (1/2\pi)\sqrt{[(C1/k^2I_0^2)C2]}$$
$$= 6.15 \text{ MHz}. \qquad (28)$$

The resonant frequency of the notch/bandpass filter can be varied merely by varying the value of the filter set current sources, which provides for an electronically tunable filter. The depth of the notch was determined to equal 0.4 uA which translates into a 42 dB notch. Further simulations were done using transistors with β values greater than 10000 and the notch depth was seen to decrease further. It is evident that in using ideal transistor models, the choice of β plays a major role in the depth that the resonant frequency is notched.

A filter with a Q = 5 and I_0 = 1 uA was simulated using real transistor models. The models used are from AT&T's CBIC-R process which is approximately a 300 MHz process. The PSpice netlist for this filter is shown in Appendix B. The notch and bandpass outputs are shown in Fig. 12. In

comparing these plots with those using ideal models in Fig. 11, it is apparent that the resonant frequency of the filter using real models is less than the filter using ideal models. This is due to the substrate capacitance of the real transistor models, which increase the effective value of C_{eff}. The set currents of this filter were then increased to 100 uA. The notch and bandpass outputs are shown in Figs. 13. The Q degradation is mainly due to the relatively small unity gain bandwidth(300MHz) of the transistor models.

The Q of the filter with I_0 = 100 uA and ideal transistor models was set equal to 10 by increasing C1 to 1 nF. The notch and bandpass outputs are shown in Fig. 14. A transient analysis of this filter was implemented with the frequency of the input sinusoid set equal to the resonant frequency of 3.07 MHz. The voltage at the notch output is shown in Fig. 15. The AC response at this node gets smaller and smaller until it should theoretically approach zero, which is the desired response of the filter. From Fig. 15 it is seen that the AC response decreases until it settles at approximately 0.07 mV. This value was seen to be a function of the timestep used in the simulation, however, this was the smallest AC response observed. This corresponds to a 34 dB notch. The discrepancy between this value and the 42 dB notch in the frequency-response analysis in Fig. 11 may be due to simulation errors in the transient analysis.

The capability of this filter to notch out multiple input sinusoids was investigated. Two sinusoids were added together at the filter input and another notch/bandpass block was placed in parallel with the existing block, as shown in Fig. 16. The Q of both blocks was set to 10 by setting C1=C4=1 nF and C2=C5=10 pF. The filter set currents for the first notch block as well as the current source I_{01} were all set to 100 uA. The set currents for the second notch block were set to 90 uA. The current source I_{015} was set to 290 uA which is equal to the total current flowing out of node 1. The resonant frequencies of the two notches are determined from eqn. 28 to be 3.07 MHz for the first notch block and 2.77 MHz for the second notch block. Ideal transistor models were used, and the frequency-response characteristic of the notch output is shown in Fig. 17. The bandpass output of the first notch block is shown on the top of Fig. 18 and the bandpass output of the second notch block is shown on the bottom of Fig. 18. It is evident that the filter notches out both sinusoids while providing enhanced versions of the sinusoids at the bandpass outputs.

A transient analysis of the filter was performed with the frequencies of the input sine waves set equal to the resonant frequencies of the notch blocks. Again the AC response at the notch output is seen to decrease and approach zero. This is shown in Fig. 19. The waveforms at the two bandpass outputs are shown in Fig. 20. It is

observed that the frequency of the sine wave at the bandpass output of the first notch block, shown at the top of Fig 20, is equal to 3.07 MHz while the frequency of the sine wave at the bandpass output of the second notch block, shown at the bottom of Fig. 20, is equal to 2.77 MHz. Thus the filter recovers the two independent sine waves. The extension of this concept to detecting and enhancing more than two sinusoids is easily accomplished by connecting additional notch filter blocks in parallel with the existing blocks.

The log domain gyrator has been shown to be a very useful component in the realisation of highpass and notch log filters. The simulation results indicate that the notch/bandpass log filter provides notch and bandpass outputs to an input sinusoid, and two independent sinusoids can be notched by adding an additional notch block in parallel.

ADAPTIVE FILTER THEORY AND AN ADAPTIVE NOTCH/BANDPASS LOG FILTER

The notch/bandpass log filter presented in the previous section is used as the basis for an adaptive notch/bandpass log filter. This filter adapts its resonant frequency to the fundamental frequency of an input sinusoid and provides both notch and bandpass responses to the sinusoid. The filter that notches
two input sinusoids described in the previous section is then modified to become an adaptive filter as well. The pertinent aspects of adaptive filter theory will first be reviewed and then applied to the log filters.

A common characteristic of nearly all applications of adaptive filtering is that some component of the problem is either unknown or changing in an unknown fashion. Adaptive filtering algorithms either provide knowledge of the unknown component or track the nature of its change. The filter described herein is of the first variety which is referred to as system identification. Figure 21 is a general outline of the system identification problem. An input x is provided to the given filter for which nothing is known except its transfer function, H:

$$H = d/x, \qquad (29)$$

where d is the desired response of the filter. The adaptive

filter also uses x as its input, and its job is to provide an output y such that y equals d, or equivalently, e = 0. Thus any parameter of the given filter can now be determined from the adaptive filter.

In most real applications a value of e=0 cannot be achieved. Instead there is some minimum value of e that the adaptive filter tries to obtain. The most reliable performance criteria for determining the error is called the mean square error or MSE. MSE is defined as the ensemble average or the expectation of the squared error sequence:

$$MSE = E[(d - y)^2], \quad (30)$$

where E[] represents the expectation operator [3].

There are many adaptive filtering algorithms that are used today. They all try to minimize the error of a filter given an input sequence. One of the most widely used algorithms is the Least Mean Square algorithm or simply the LMS algorithm. The LMS algorithm recursively updates the adapting parameters until the minimum error is achieved. The algorithm states that the current value of the adapting parameters is equal to the previous value of these same parameters plus the scaled product of the previous error value and the previous input. This is represented by;

$$W_N(n + 1) = W_N(n) + \alpha e(n) X_N(n) \quad (31)$$

where $W_N(n + 1)$ is an N-length vector representing the updated parameter values, $W_N(n)$ is an N-length vector representing the previous parameter values, $X_N(n)$ is an N-

length vector representing the input sequence, e(n) is the scalar error value, and α is called the gain constant of the filter. The reader is referred to [4] for a detailed derivation of the LMS algorithm.

The fact that a value of e=0 is usually not obtainable means that the filter parameters will fluctuate around their optimum values with some degree of noise. This is referred to as misadjustment noise. A tradeoff exists between the misadjustment noise of the filter and the speed at which the filter converges to its optimum value. This can be controlled by the choice of α. As α is increased, the rate of convergence will increase but the amount of misadjustment noise will also increase. As α is decreased the amount of misadjustment noise decreases but it takes longer for the filter to reach its optimum value.

A fundamental property of minimum MSE filters is the orthogonality conditions. This property states that after the adaptive filter has converged to its optimum value, the expectation of the product of the error and the input is zero, or:

$$E[x(n)e(n)] = 0. \qquad (32)$$

From the definition of orthogonality, x(n) and e(n) must then be orthogonal.

What follows herein is a description of an adaptive filter which adapts its resonant frequency to the fundamental frequency of an input sinusoid and provides both

a notch and a bandpass response of the sinusoid. Modifications are made to the notch/bandpass log filter shown in Fig. 8 to achieve the adaptivity.

In this case the desired response of the filter is to have the notch output equal zero. Referring to Fig. 21, d should be set to zero and the notch output of the filter should be considered y. However, since d = 0, and the error e = d - y, the notch output is also the error of the filter. Therefore the problem that presents itself is how to achieve a signal that is orthogonal to the input signal only at the resonant frequency of the filter. We will call this signal the gradient signal and it would replace e(n) in the orthogonality conditions in eqn. 32.

It would seem logical that additional circuitry should be designed to produce such a signal. However, it is observed that this signal already exists in the filter. From Fig. 10, this signal exists at node 3, the voltage on capacitor C2. It is clear that the bandpass voltage at node 2 is in phase with the input only at the resonant frequency of the filter. The voltage at node 3 is 90 degrees out of phase with the voltage at node 2 due to capacitor C2. Thus the voltage at node 3 will be orthogonal to the input only at the resonant frequency of the filter, and the orthogonality conditions will hold true if this signal is multiplied by the input and the expectation of the product is taken. Fig. 22 shows a plot of the phase of node 2, the

log bandpass output, versus frequency, where the resonant frequency, f_r, is the frequency at which the phase equals zero. The phase response at node 3 is shown in Fig. 23. It is clear that the phase of node 3 will be orthogonal to the input signal only at the resonant frequency, f_r.

PSpice was used to multiply the voltage at node 3 by the input voltage, which was acquired by means of a 0V DC voltage source at the input used to sense the input current. A current-controlled voltage source was then used to transform this current into a voltage of the same magnitude. A polynomial dependent voltage-controlled current source is used to multiply these two voltages and transform the product into a current of the same magnitude. This current is then placed through an integrator to achieve the expectation operation. The integrator is comprised of a capacitor in parallel with a very large resistor.

With discrete-time sequences, the expectation operation can be depicted as a sum;

$$E = \Sigma\ [x(n) * e(n)]. \qquad (33)$$

With continous-time signals, integration is equivalent to taking the expectation. This subject has been covered in the literature and the reader is referred to [5]. The voltage on capacitor C4 is then seen to be the expectation of the error signal and the input signal;

$$E[x(t) * e(t)] = 1/C4 \int [x(t) * e(t)]\ dt. \qquad (34)$$

In this case e(t) is represented by the previously mentioned

gradient signal.

The filter is made to be adaptive by placing voltage-controlled current sources at the filter set currents to transform the voltage on capacitor C4 into currents. The adaptation process is illustrated in Fig. 24. The filter adjusts these currents to minimize the notch output. To do this the voltage at node 3 has to be changing in such a way that, when multiplied by the input current, the product, when integrated, approaches the value in volts of the filter notch set current in amps. This occurs by the phase of the voltage at node 3 adjusting until it is 90 degrees out of phase with the input signal.

From eqn. 34, it is apparent that the quantity 1/C4 represents the gain constant, α, of the adaptive filter. Thus as C4 is increased, α is decreased and the filter will display less misadjustment noise but will take longer to converge. On the other hand, if C4 is decreased, α is increased and the filter will converge at a greater rate but will display more misadjustment noise. The schematic which incorporates these adaptation characteristics into the notch/bandpass log filter is seen in Fig. 25.

The adaptive filter in Fig. 25 was simulated under the following conditions. The input sine wave was given a frequency of 6.15 MHz which is the resonant frequency that corresponds to an optimum filter set current value of 100 uA, from eqn. 28. An initial voltage of 99 uV was placed on

capacitor C4 so that the filter set currents and current source G1 would start out at 99 uA. C4 was chosen to be 10 nF and a Q of 5 was used. The PSpice netlist is shown in Appendix C. The results of the simulation are shown in Figs. 26-29. Fig. 26 displays the current through current source G1. This waveform is representative of the waveforms at all of the filter set currents since all of these were set up as voltage-controlled current sources with a gain factor of 1. As is seen, the current adapts from 99 uA to 100 uA in approximately 4 uS. The set currents approach their optimum value of 100 uA in an exponential fashion. Approximately 1 uA of misadjustment noise is observed after the filter has converged. The top of Fig. 27 shows the nonlinear log notch voltage and the bottom of Fig. 27 shows the exponentiated notch output voltage. The AC values of these parameters are not zero due to the large amount of misadjustment noise seen in the set current adaptation shown in Fig. 26. Fig. 28 shows the corresponding log and exponentiated bandpass voltages.

As mentioned earlier, the product of the gradient signal, the voltage at capacitor C2, and the input voltage was converted to a current and used as an integrator along with capacitor C4. It is interesting to note that the gradient signal varies its phase until it is 90 degrees out of phase with the input voltage when the set currents reach their optimum values of 100 uA. As previously explained,

this is due to the orthogonality conditions and is a necessary characteristic of an adaptive filter. The gradient signal is shown at the top of Fig. 29 and the input voltage is shown at the bottom of Fig. 29.

The gain constant of the adaptive filter was then decreased by increasing C4 to 100 nF. This results in the filter taking longer to converge while displaying less misadjustment noise. The filter set current waveform is shown at the top of Fig. 30 and the notch output is shown at the bottom of Fig. 30. This notch output is seen to be less than the notch output with C4 = 10 nF shown in Fig. 26. This AC response would decrease to zero if C4 is increased significantly. However the increasingly longer simulation times that result make this impractical to display. It takes the filter approximately 100 uS to converge but the amount of misadjustment noise is approximately 0.1 uA, or 1/10 the amount observed with C4=10 nF.

The initial conditions were then changed so that the currents would start out at 70 uA. C4 was set equal to 5 nF. Fig. 31 shows that the filter adapts to its optimum value in approximately 60 uS. Fig. 32 shows that when the set currents start out at 130 uA, the filter takes approximately 50 uS to converge.

Simulations were run with real models with I_0 = 100 uA and an input sinusoid of frequency equal to 5.6 MHz. This is approximately the resonant frequency of the non-adaptive

notch/bandpass log filter using real models with I_0 = 100 uA. A Q of 5 was used. The set currents started out at 98 uA and are seen to converge to approximately 100.5 uA, as shown in Fig. 33. C4 was set equal to 2 nF in this simulation.

The adaptive characteristics of the filter that notches two input sinusoids were then investigated. A second integrator is used for the second notch block, as shown in Fig. 34. This integrator is comprised of GX2, C7, and R3. Voltage-controlled current sources are placed at the set currents of the second notch block with values in amps equal to v(int2), the voltage on capacitor C7, in volts. The Q of both notch blocks was set equal to 10 by setting C1=C5=1 nF and C2=C6=10 pF. The frequencies of the two input sinusoids were set to 3.07 MHz and 2.77 MHz. From eqn. 28 these are the resonant frequencies that correspond to set current values of 100 uA and 90 uA, respectively. The gain constants of the two blocks were set equal by setting C4=C7=40 nF.

The filter was simulated with initial set current values of 98 uA and 88 uA for the two notch blocks. The results are shown in Figs. 35 and 36. The top of Fig. 35 shows the current through current source G1 which is equivalent to the set currents in the first notch block. The bottom of Fig. 35 shows the current through current source G9 which is equivalent to the set currents in the

second notch block. It is observed that both of these currents converge to their optimum values of 100 uA and 90 uA, respectively. Fig. 36 shows the voltage waveforms at the bandpass outputs of each notch block. The voltage at the bandpass output of the first notch block on the top of Fig. 36 has a frequency of 3.07 MHz while the voltage at the bandpass output of the second notch block on the bottom of Fig. 36 has a frequency of 2.77 MHz. Thus the two independent input sinusoids are recovered in a linearly filtered form.

The initial conditions of the filter were then changed so that the set currents of the first notch block start at 85 uA and the set currents of the second notch block start at 89 uA. Fig. 37 shows that both set currents converge to their optimum values in approximately 70 uS.

Adaptive filter theory has been implemented in the design of an adaptive notch/bandpass log filter that adapts its resonant frequency to the frequency of an input sinusoid. Simulations have been presented which indicate that this filter adapts under a number of different initial conditions with varying levels of misadjustment noise and adaptation rates, dependent on the choice of capacitor C4.

CONCLUSION

The concepts of log filter theory and adaptive filter theory have been brought together in this work to achieve the design of a continuous-time adaptive log filter. Initially a first order lowpass log filter was presented. The extension of this filter to a first order highpass log filter is made through the use of a log domain gyrator. Two log domain gyrators are then implemented in the design of a notch/bandpass log filter. This filter forms the basis for an adaptive notch log filter. The filter is able to adapt to very high frequency signals due to the fact that log filters process signals nonlinearly while maintaining an overall linear transfer function. Moreover, because the only active elements in the filter are current mirrors, the complexity of the filter is very low compared to discrete-time adaptive filters.

The simulation results presented indicate that this adaptive log filter could be quite useful in many signal processing applications, the most notable being those which involve the detection and enhancement of sinusoidal signals. It has been shown that with the addition of parallel filter sections the filter is able to adapt to multiple sinusoidal inputs. The filter design lends itself quite well to its implementation in monolithic form. The only further

requirement would be the design of an effective multiplier to multiply the gradient signal and the input signal, this being one step of the adaptation process.

REFERENCES

1. D.R. Frey, "Log-Domain Filtering: An Approach to Current-mode Filtering", IEE Proc. Pt. G, vol. 140, no. 6, pp. 406-416, Dec. 1993.

2. D.R Frey, "A Log Domain Gyrator and New Filter Topologies", Personal Correspondence.

3. A. Papoulis, *Probability, Random Variables, and Stochastic Processes,* McGraw-Hill, New York, 1984.

4. S. Thomas Alexander, *Adaptive Signal Processing, Theory and Applications,* Springer-Verlag, New York, 1986.

5. T. Kwan and k. Martin, "An Adaptive Algorithm for IIR Filters," Proc. IEEE, vol. 66, pp. 585-588, May 1978.

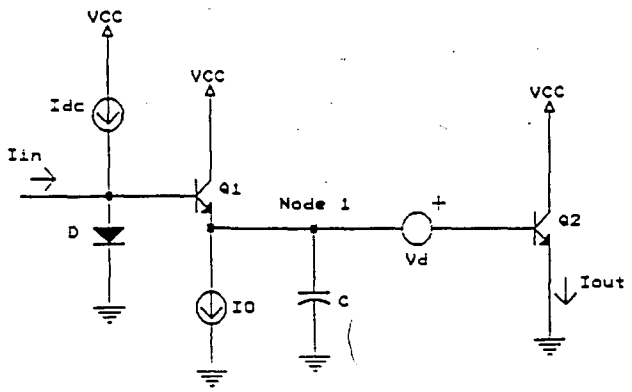

FIG. 1 – 1ST ORDER LOWPASS LOG FILTER, SIMPLIFIED SCHEMATIC

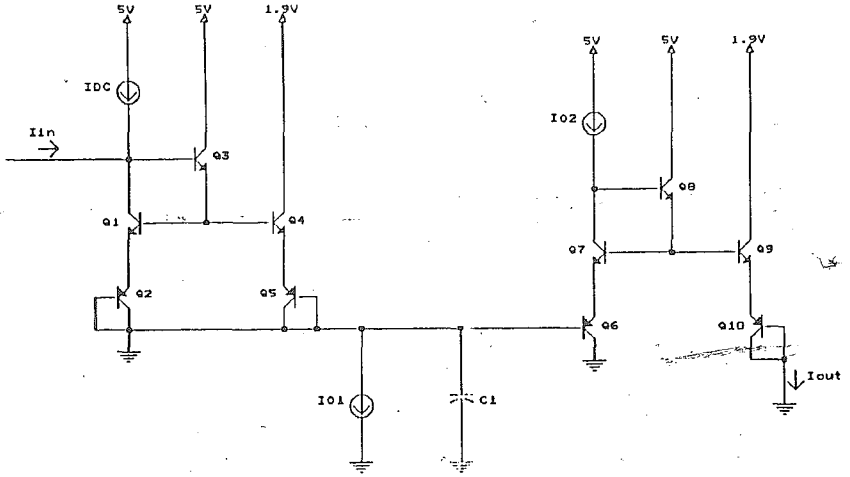

FIG. 2 – 1ST ORDER LOWPASS LOG FILTER, COMPLETE SCHEMATIC

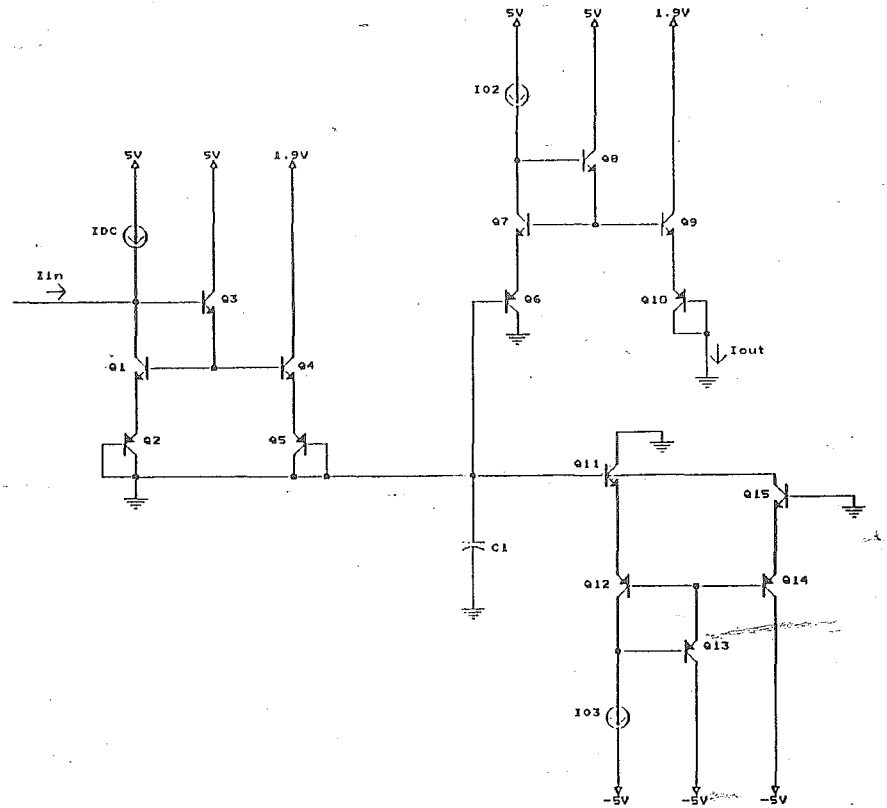

FIG. 3 - IDEAL INTEGRATOR

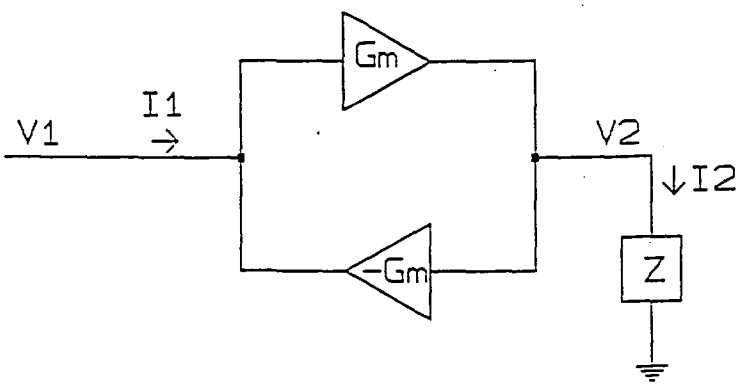

FIG. 4 - LINEAR GYRATOR

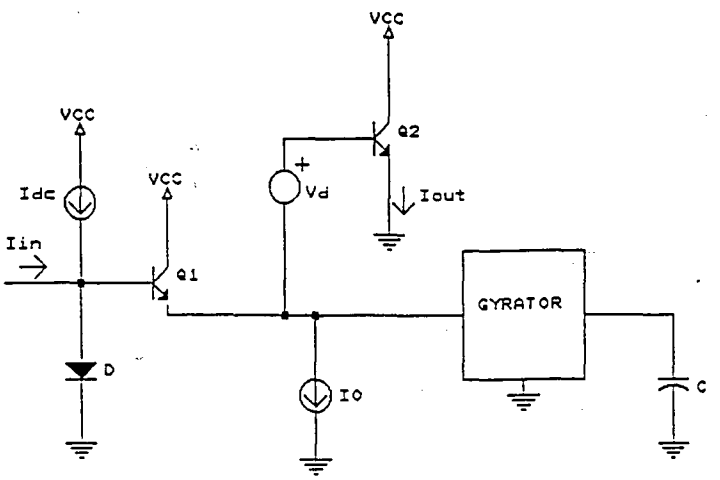

FIG. 5 – 1ST ORDER HIGHPASS LOG FILTER, SIMPLIFIED SCHEMATIC

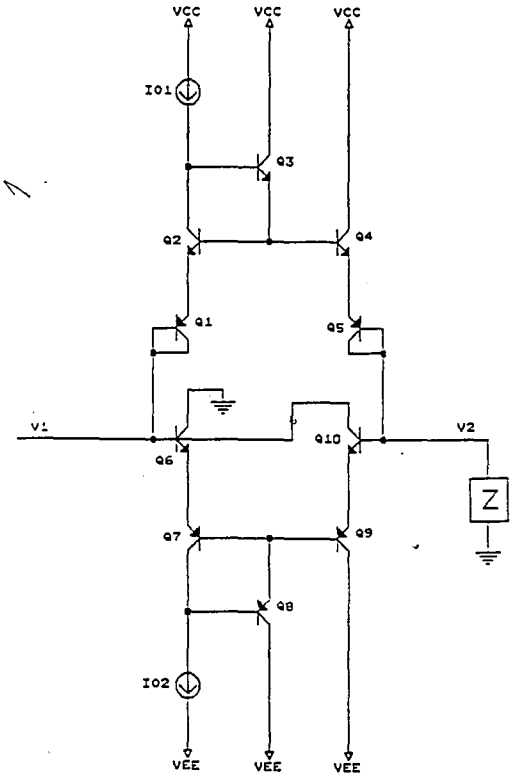

FIG. 6 - LOG DOMAIN GYRATOR

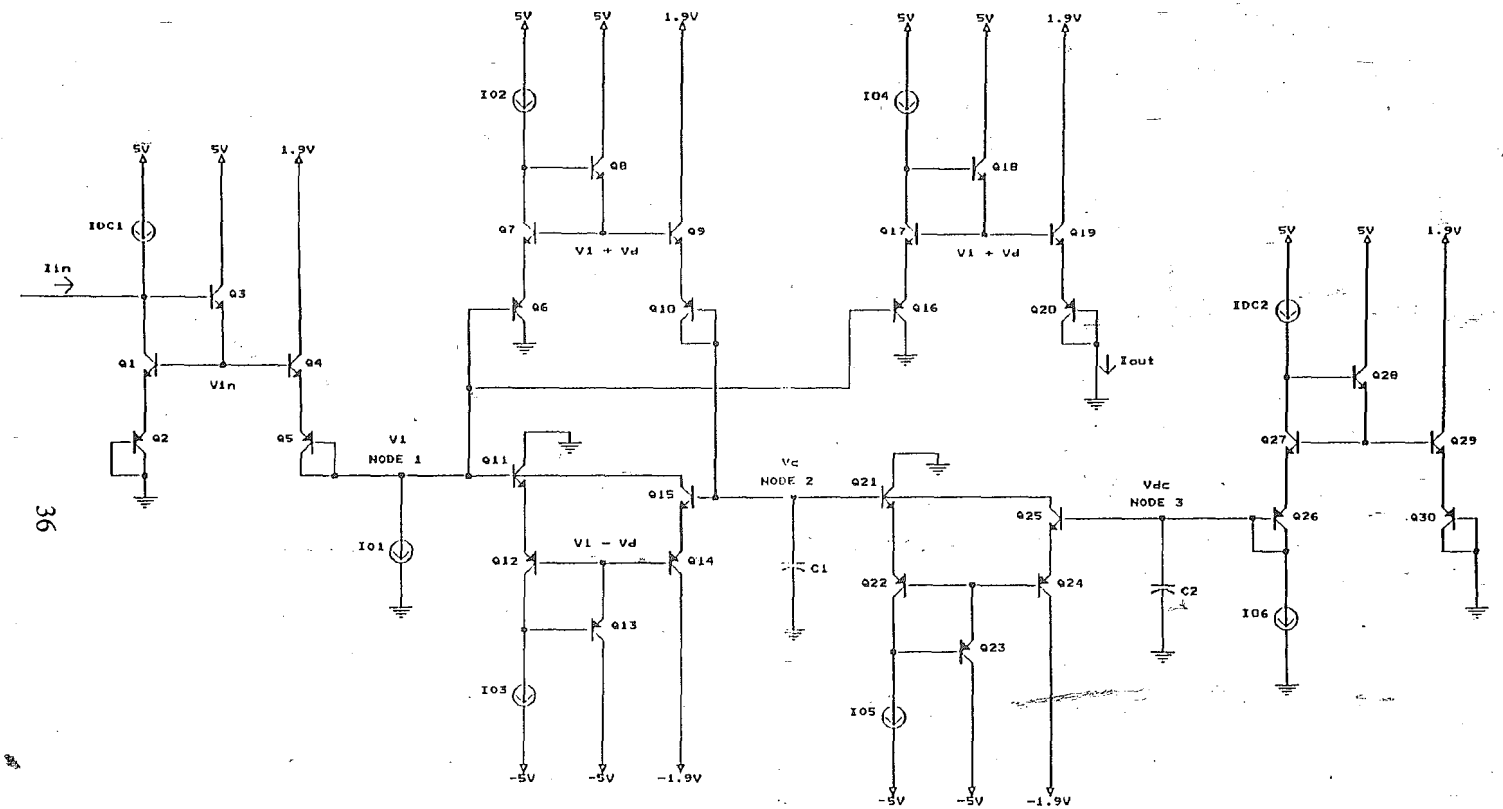

FIG. 7 - 1ST ORDER HIGHPASS LOG FILTER, COMPLETE SCHEMATIC

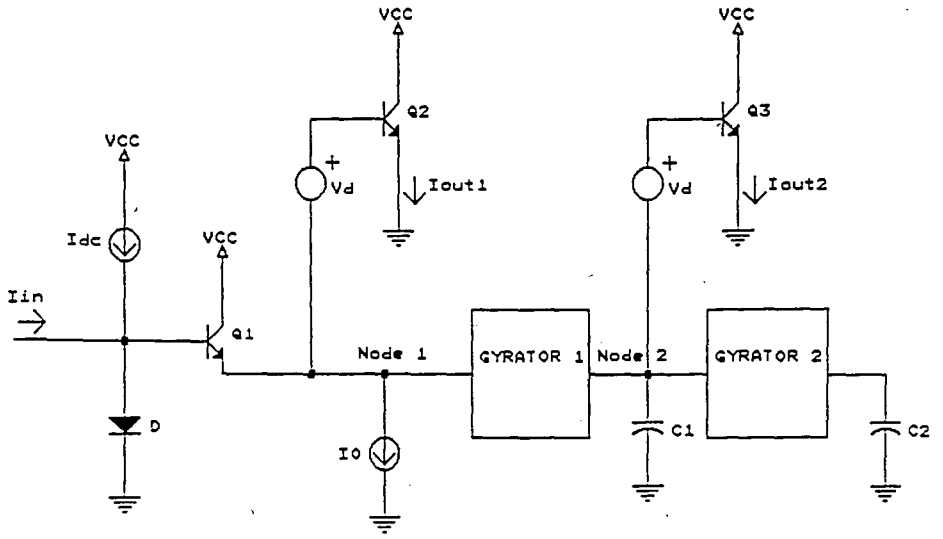

FIG. 8 – NOTCH/BANDPASS LOG FILTER, SIMPLIFIED SCHEMATIC

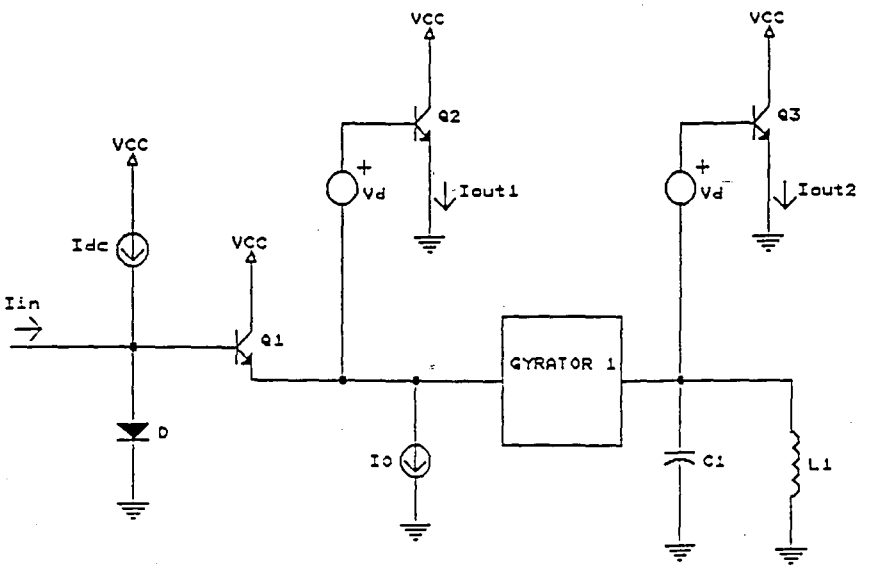

FIG. 9 – NOTCH/BANDPASS LOG FILTER, GYRATOR 2 REPLACED BY L1

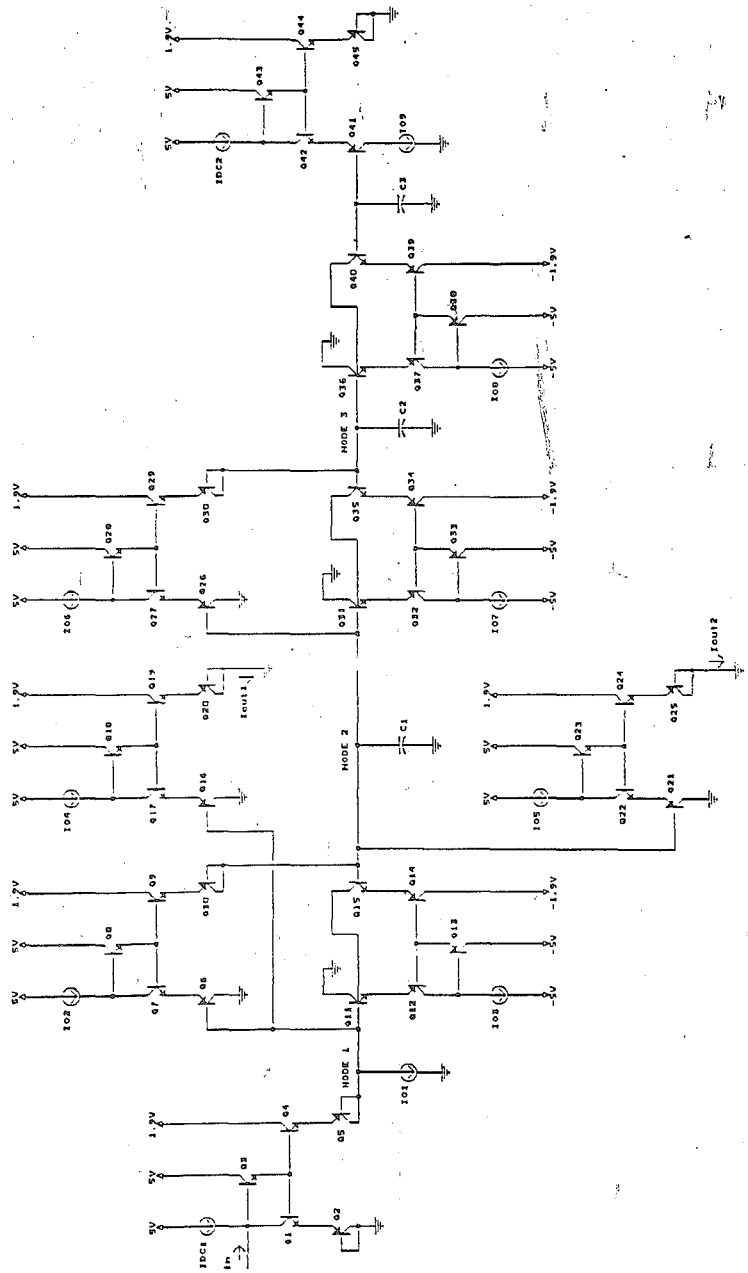

FIG. 10 - NOTCH/BANDPASS LUG FILTER, COMPLETE SCHEMATIC

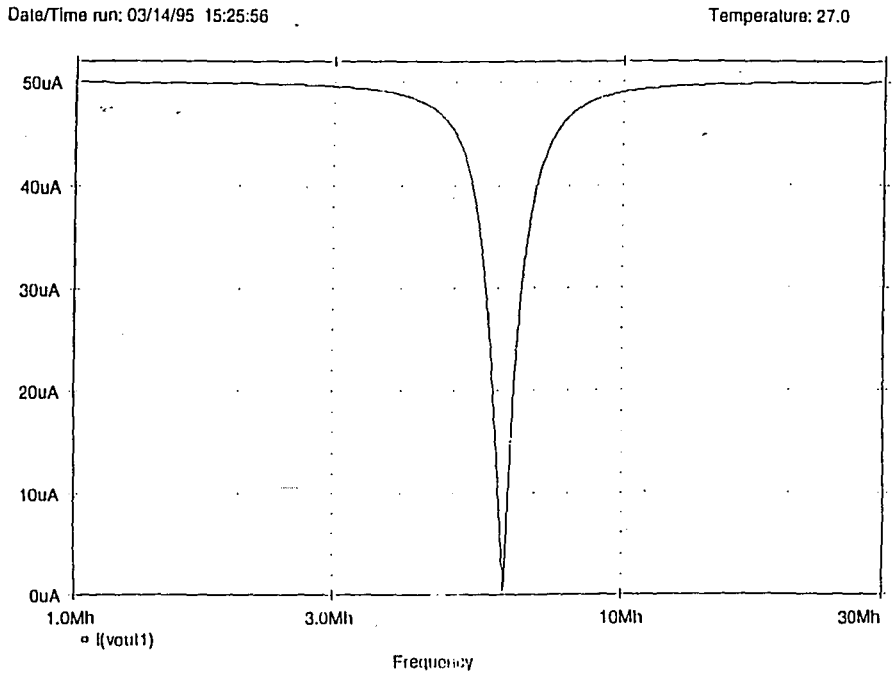

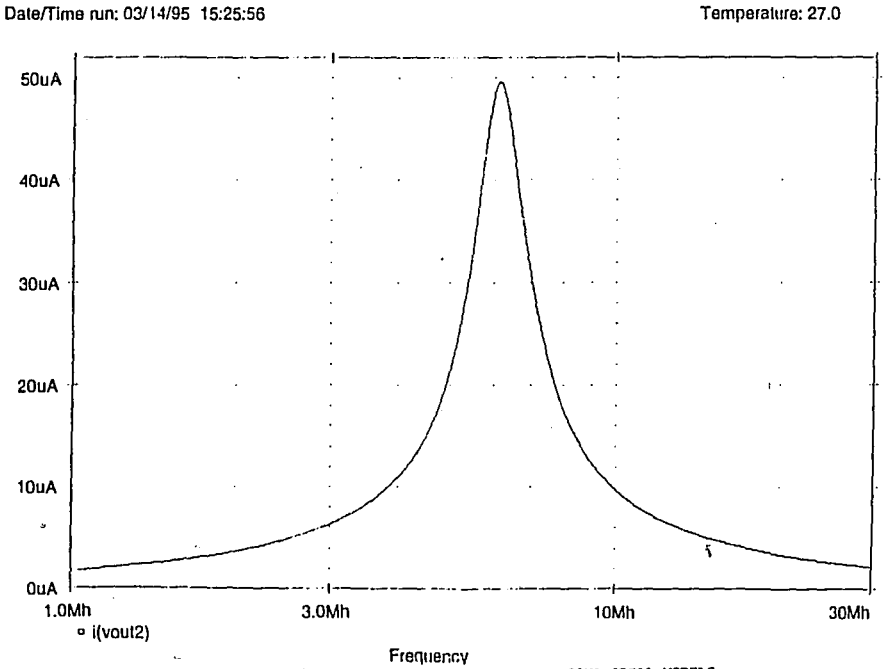

FIG. 11 - NOTCH/BANDPASS LOG FILTER, Q=5, I_o=100UA, IDEAL MODELS, NOTCH AND BANDPASS OUTPUTS

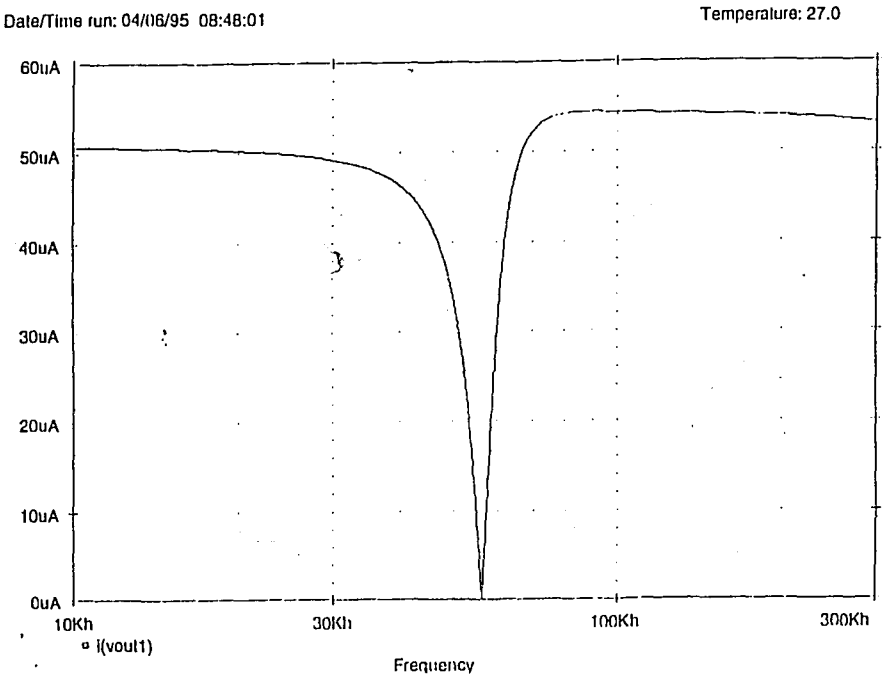

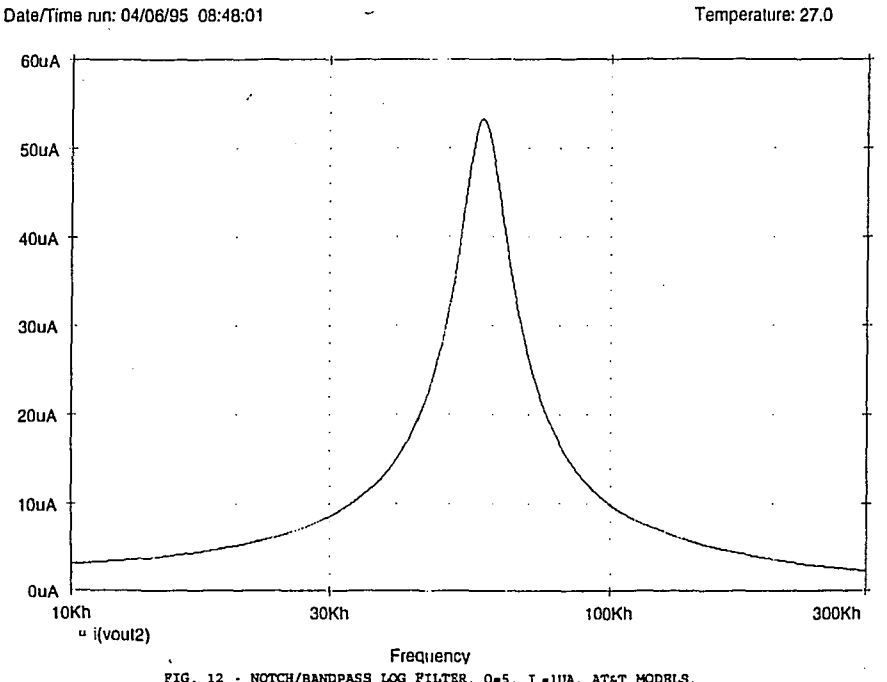

FIG. 12 - NOTCH/BANDPASS LOG FILTER, Q=5, I_o=1UA, AT&T MODELS, NOTCH AND BANDPASS OUTPUTS

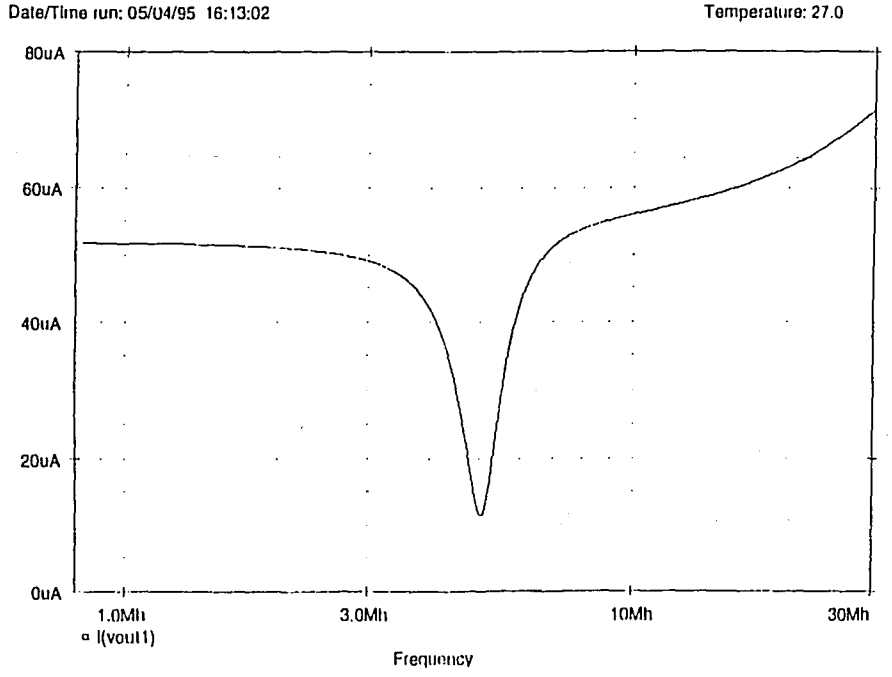

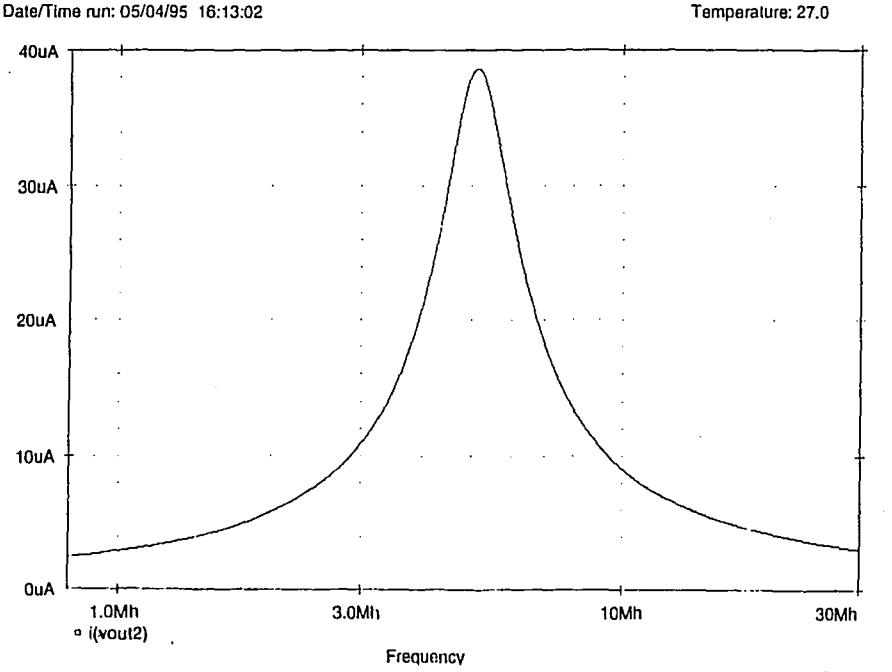

FIG. 13 - NOTCH/BANDPASS LOG FILTER, Q=5, I_0=100UA, AT&T MODELS, NOTCH AND BANDPASS OUTPUTS

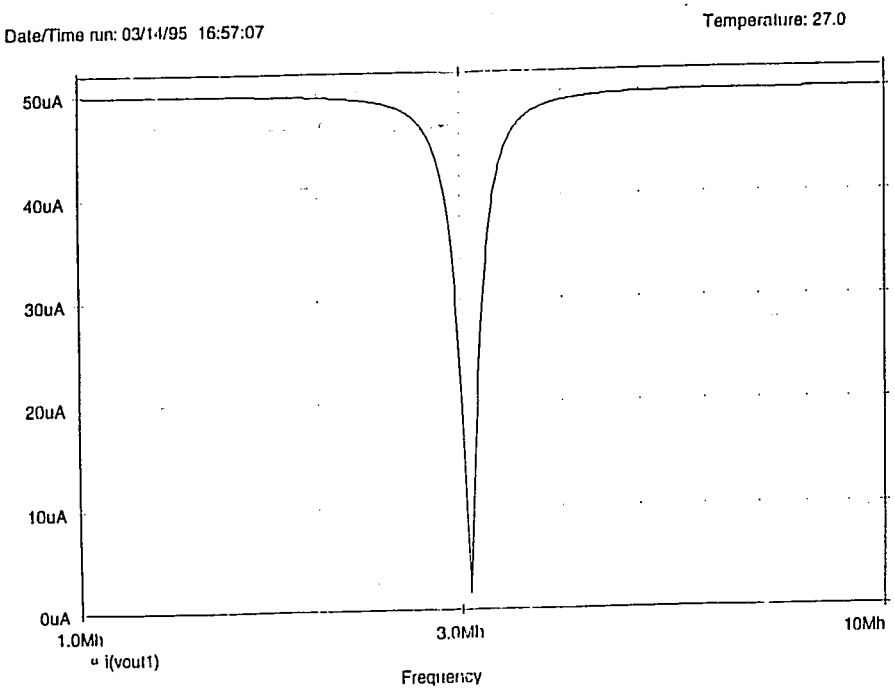

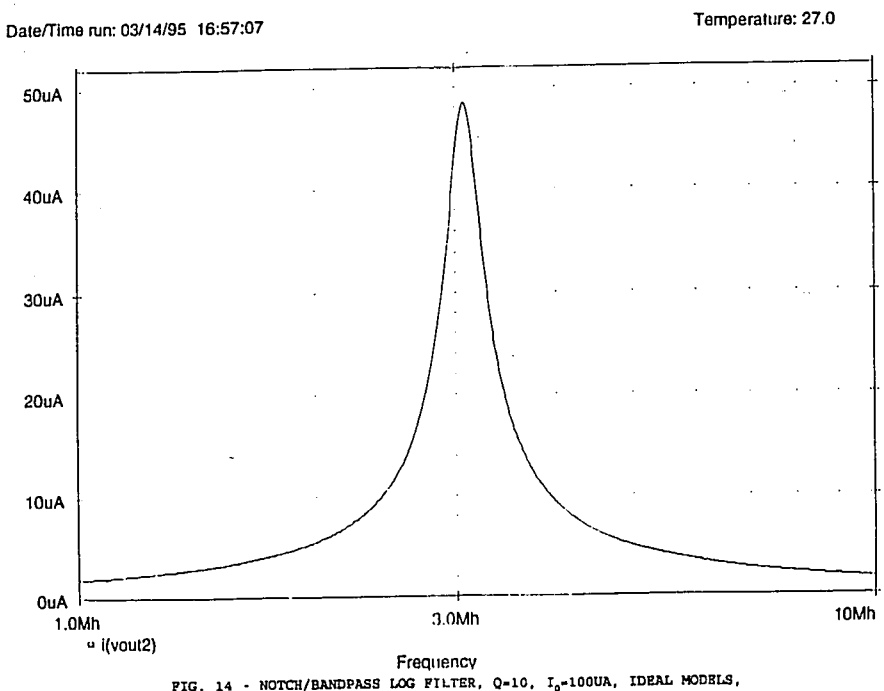

FIG. 14 - NOTCH/BANDPASS LOG FILTER, Q=10, I_o=100UA, IDEAL MODELS, NOTCH AND BANDPASS OUTPUTS

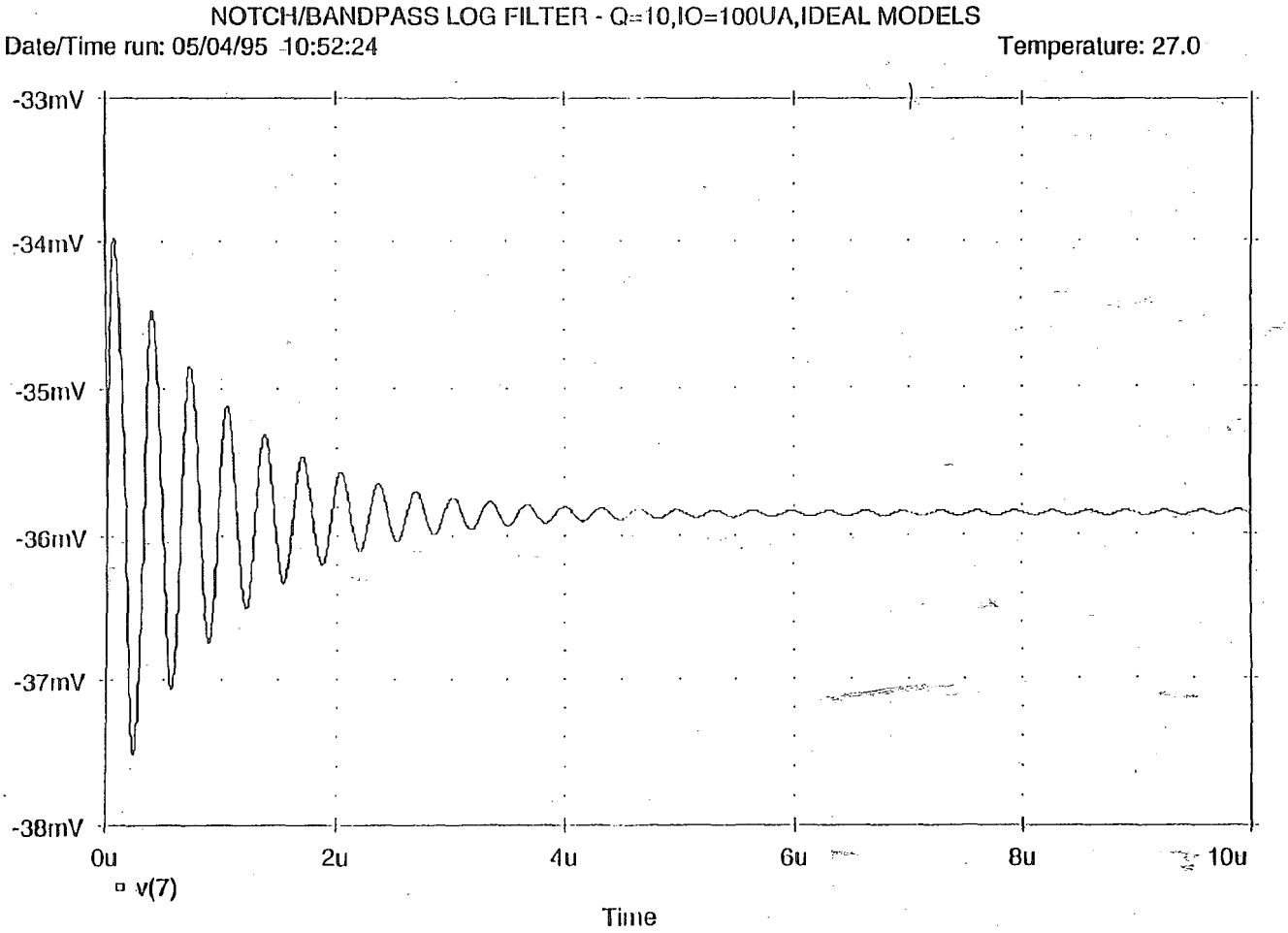

FIG. 15 - NOTCH/BANDPASS LOG FILTER, Q=10, I_o=100UA, IDEAL MODELS, NOTCH OUTPUT TRANSIENT RESPONSE

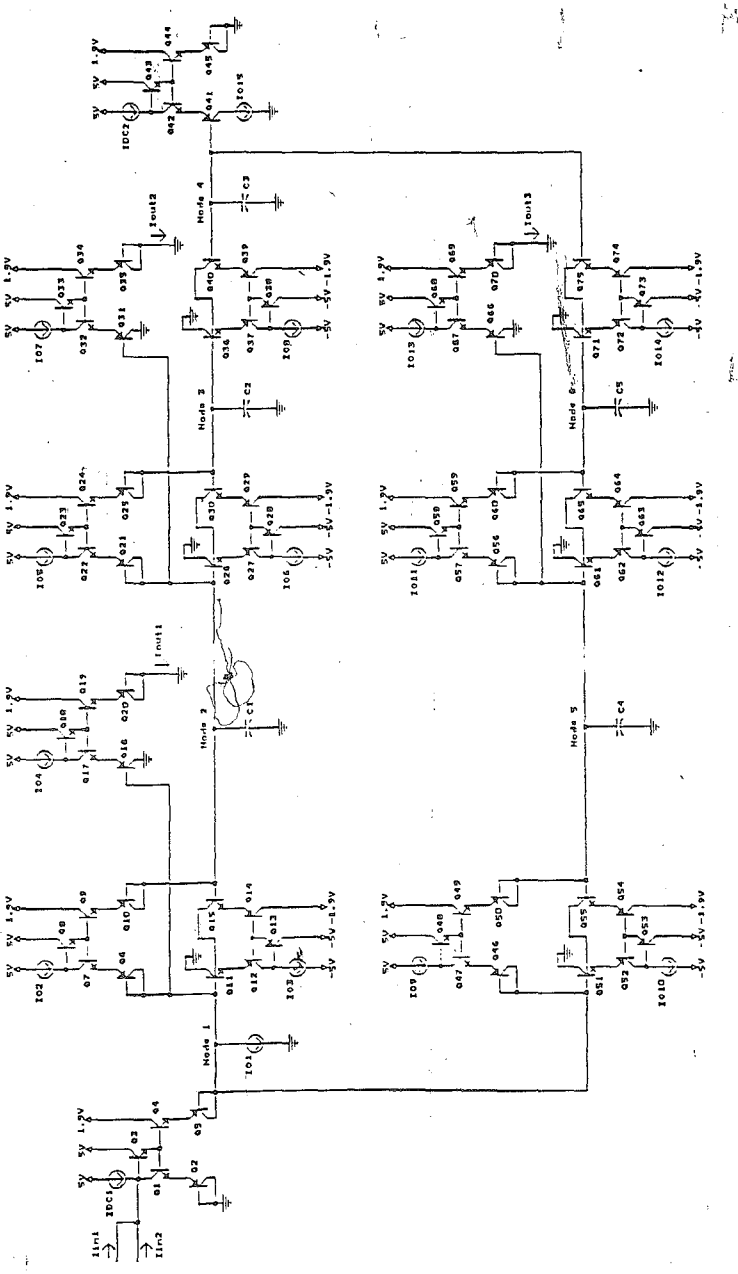

FIG. 16 - NOTCH/BANDPASS LOG FILTER, 2 INPUT SINUSOIDS

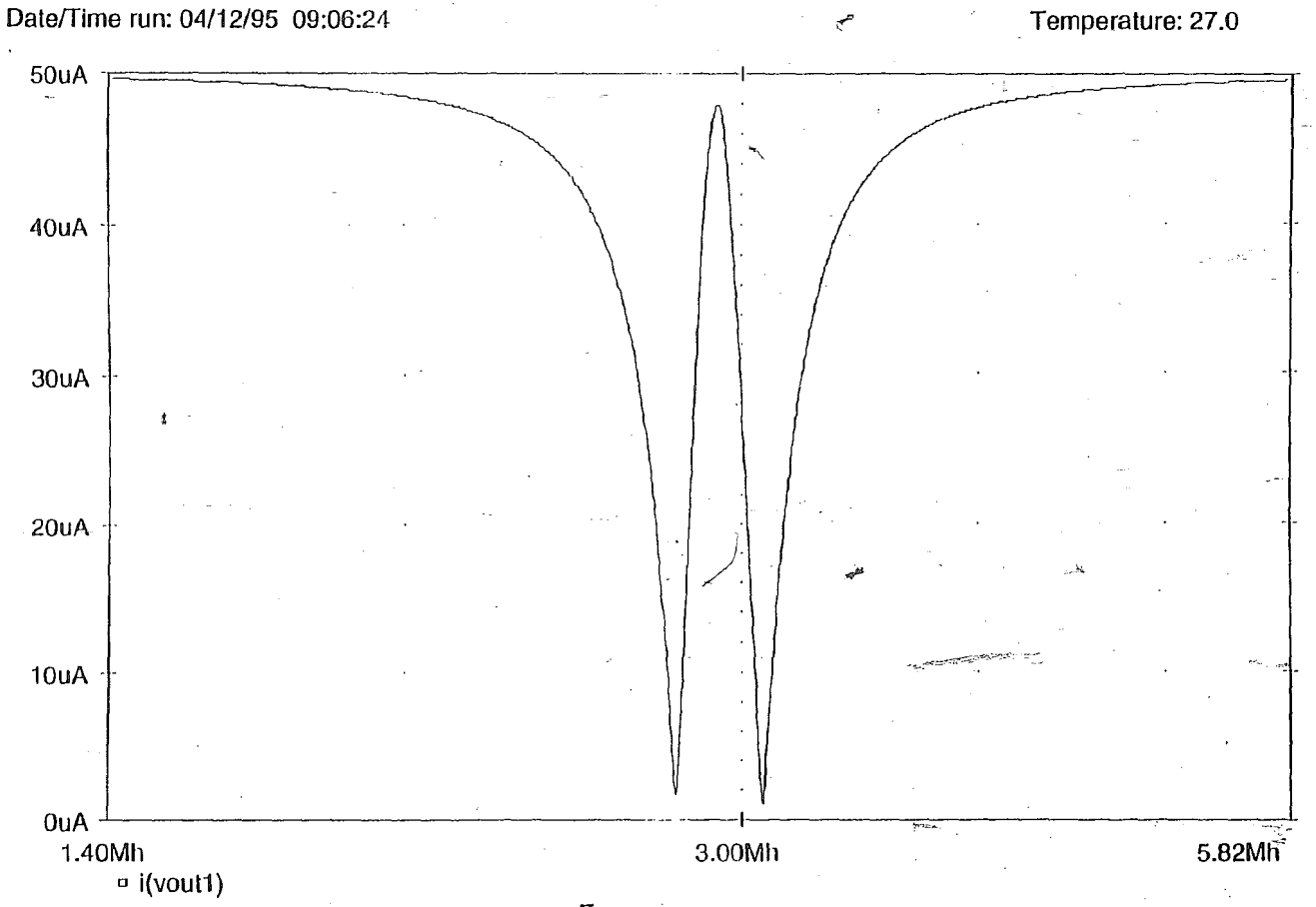

FIG. 17 - NOTCH/BANDPASS LOG FILTER, 2 NOTCH BLOCKS, I_o1=100UA, I_o2=90UA, IDEAL MODELS, NOTCH OUTPUT

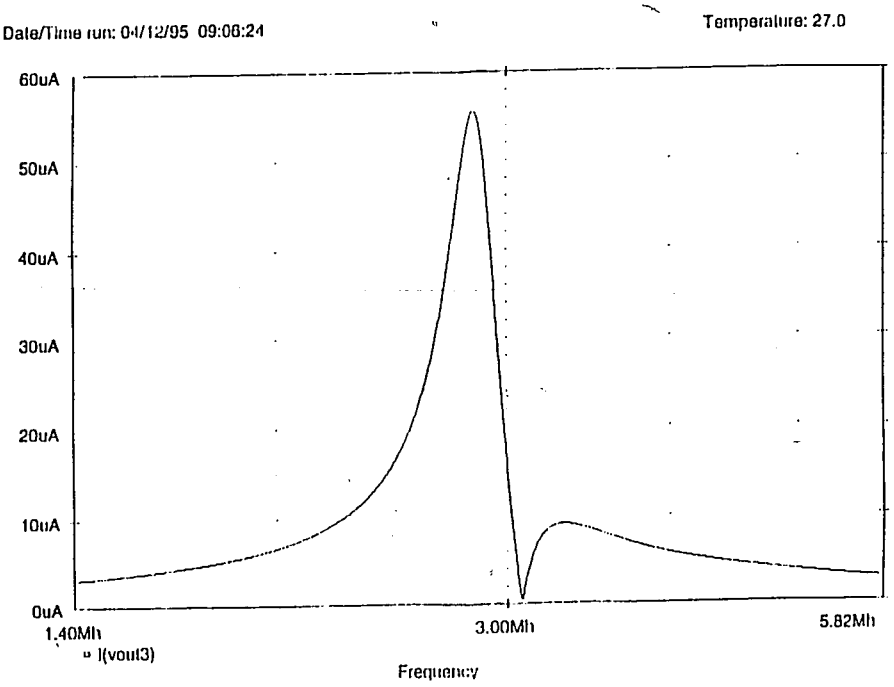

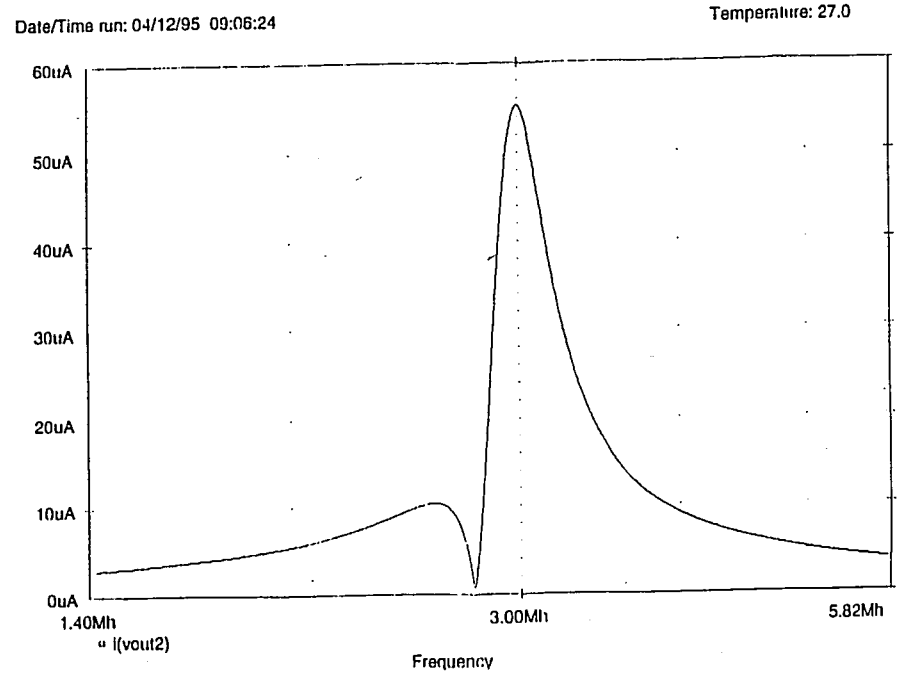

FIG. 18 - NOTCH/BANDPASS LOW FILTER, 2 NOTCH BLOCKS, IO1=100UA, IO2=99UA, IDEAL MODELS, BANDPASS OUTPUTS

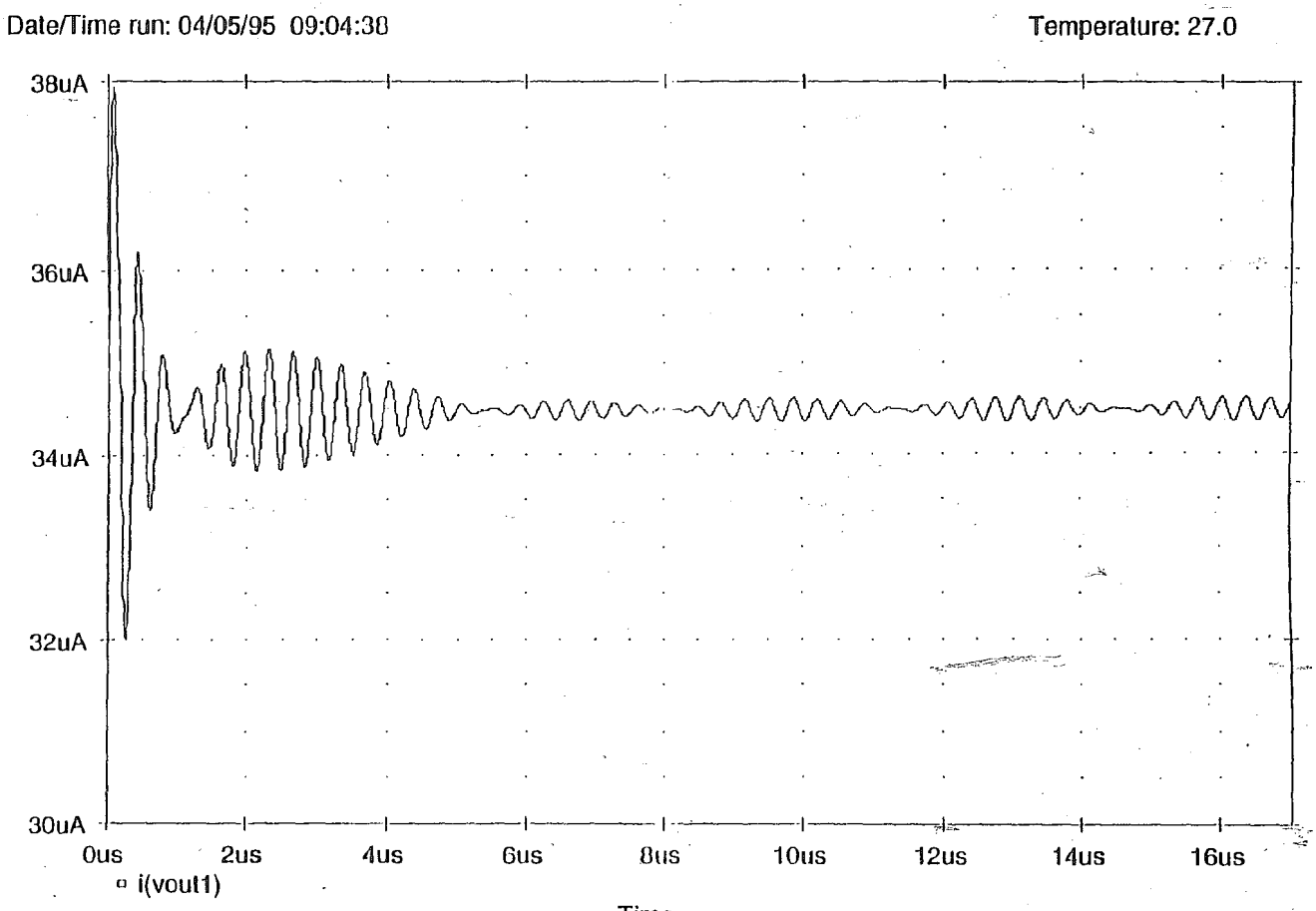

FIG. 19 - NOTCH/BANDPASS LOG FILTER, 2 NOTCH BLOCKS, I_{01}=100UA, I_{02}=90UA, IDEAL MODELS, NOTCH OUTPUT TRANSIENT RESONSE

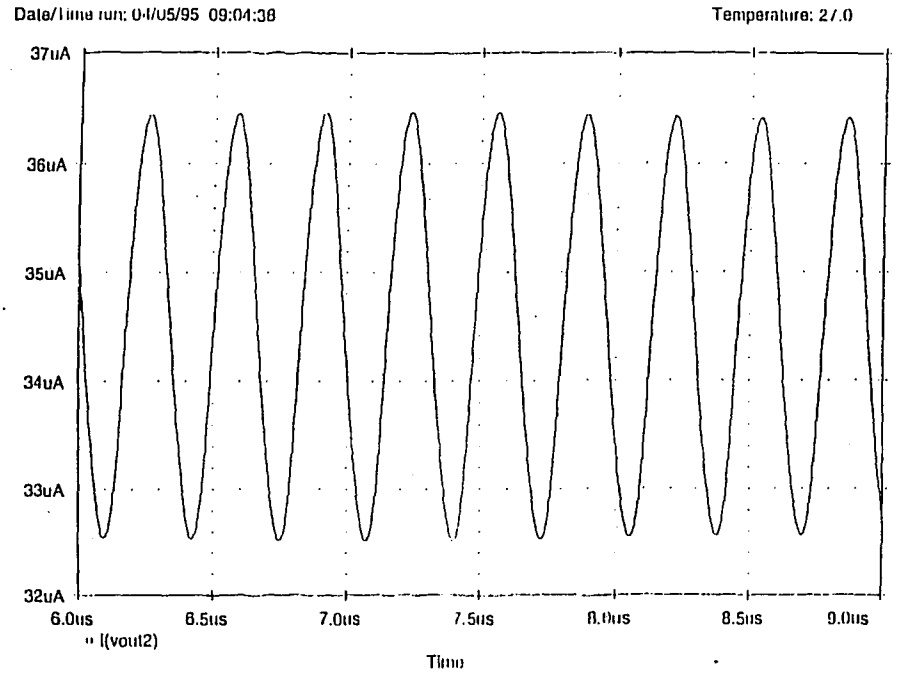

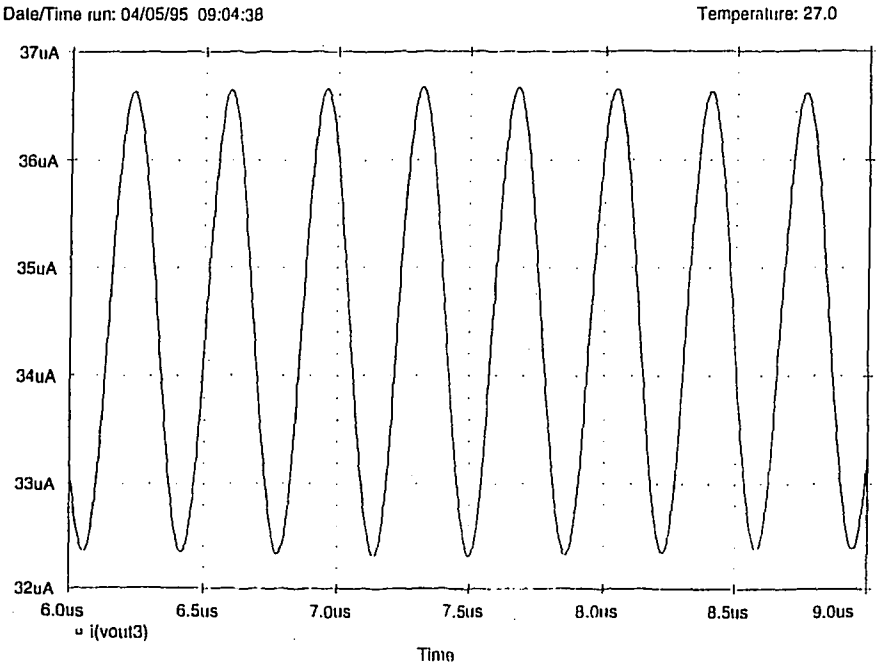

FIG. 20 - NOTCH/BANDPASS LOG FILTER, 2 NOTCH BLOCKS, I_{BI}=100UA, I_{BW}=50UA, IDEAL MODELS, BANDPASS OUTPUTS TRANSIENT RESPONSE

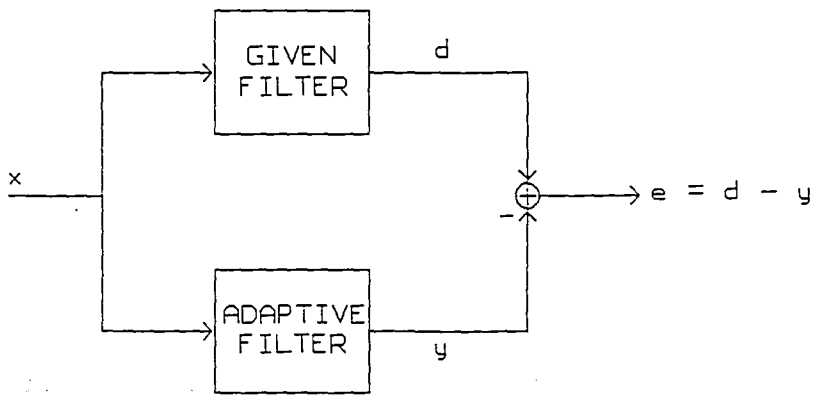

FIG. 21 – SYSTEM IDENTIFICATION

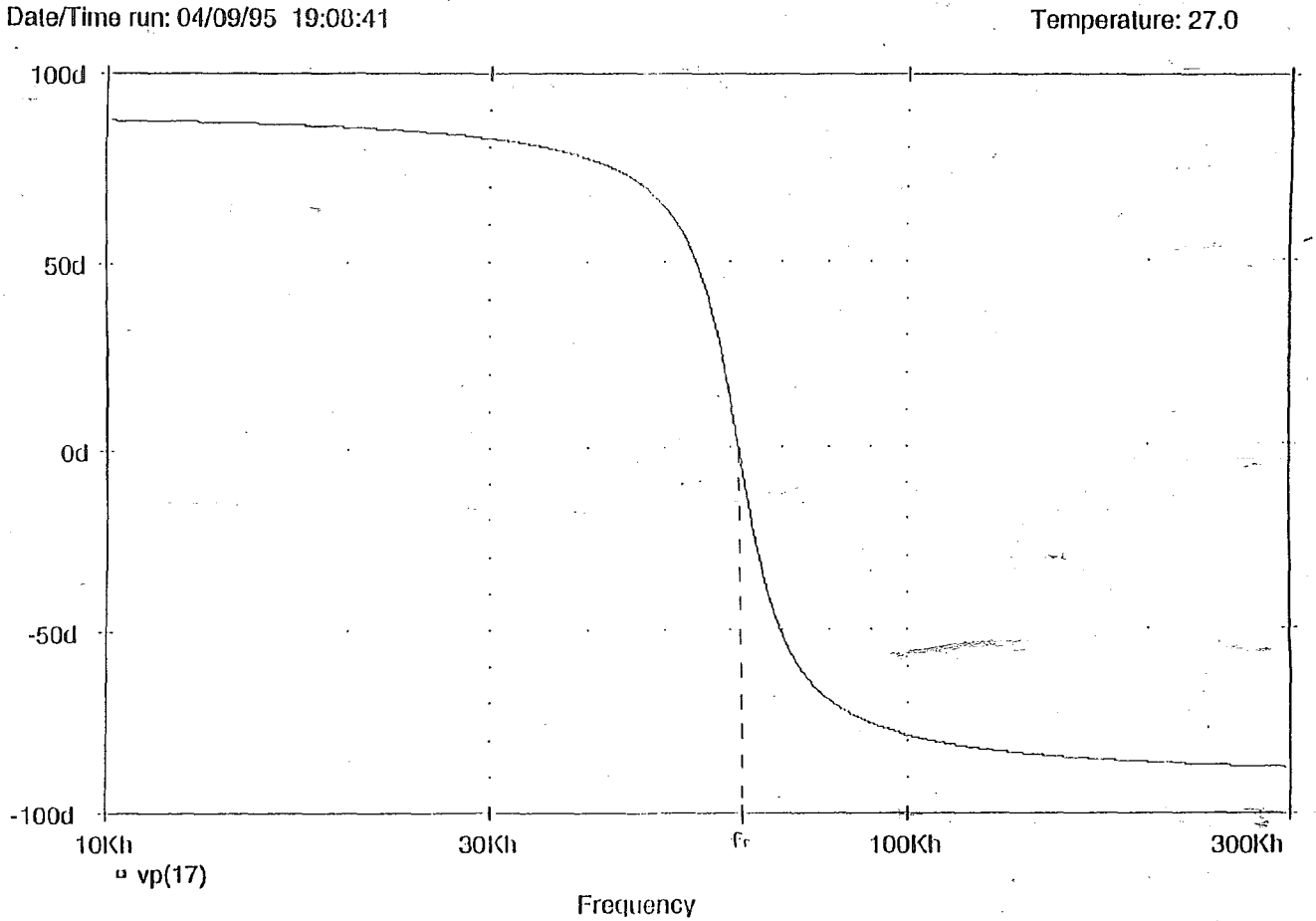

FIG. 22 - NOTCH/BANDPASS LOG FILTER, FREQUENCY RESPONSE AT BANDPASS NODE

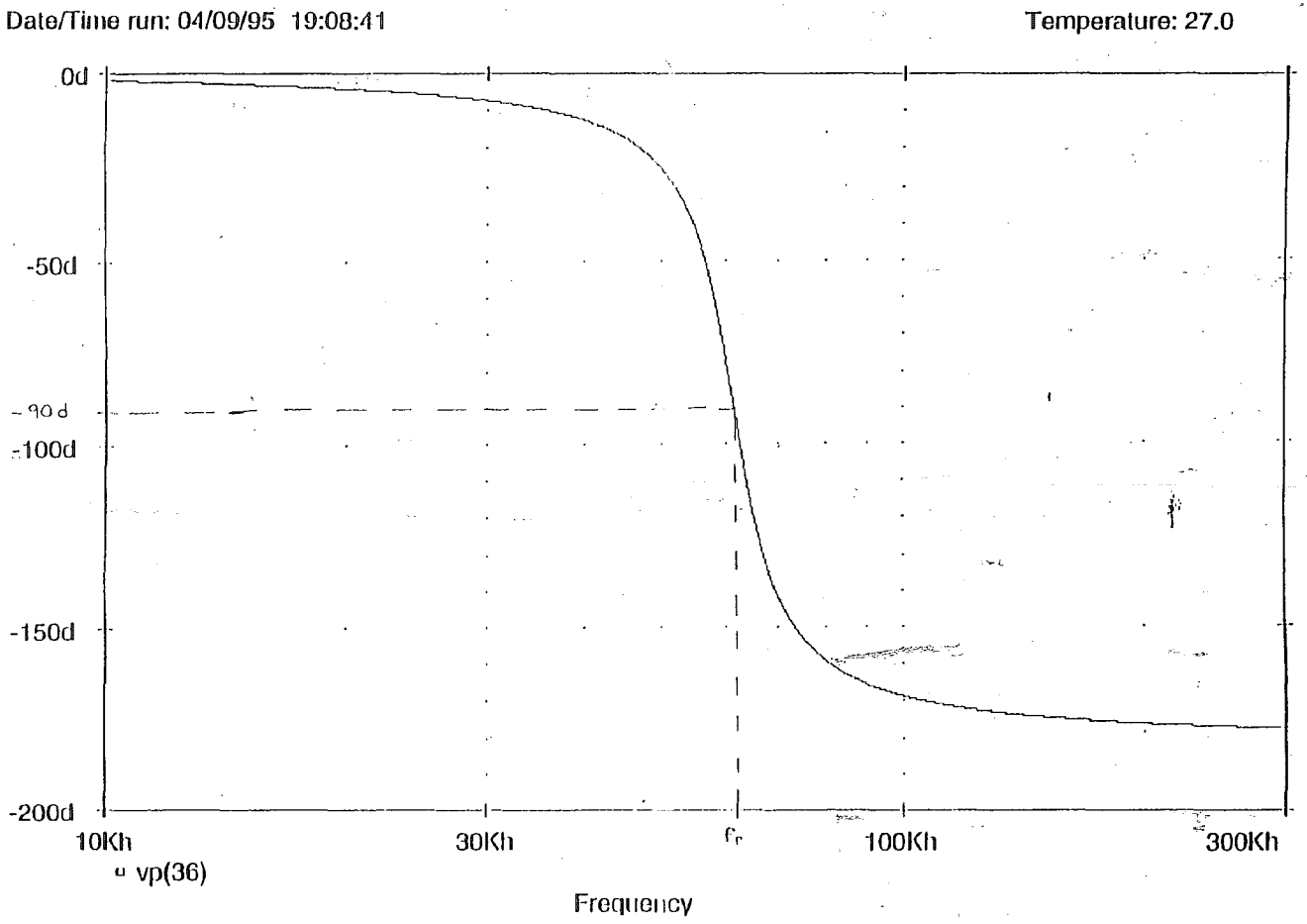

FIG. 23 - NOTCH/BANDPASS LOG FILTER, FREQUENCY RESPONSE OF GRADIENT SIGNAL

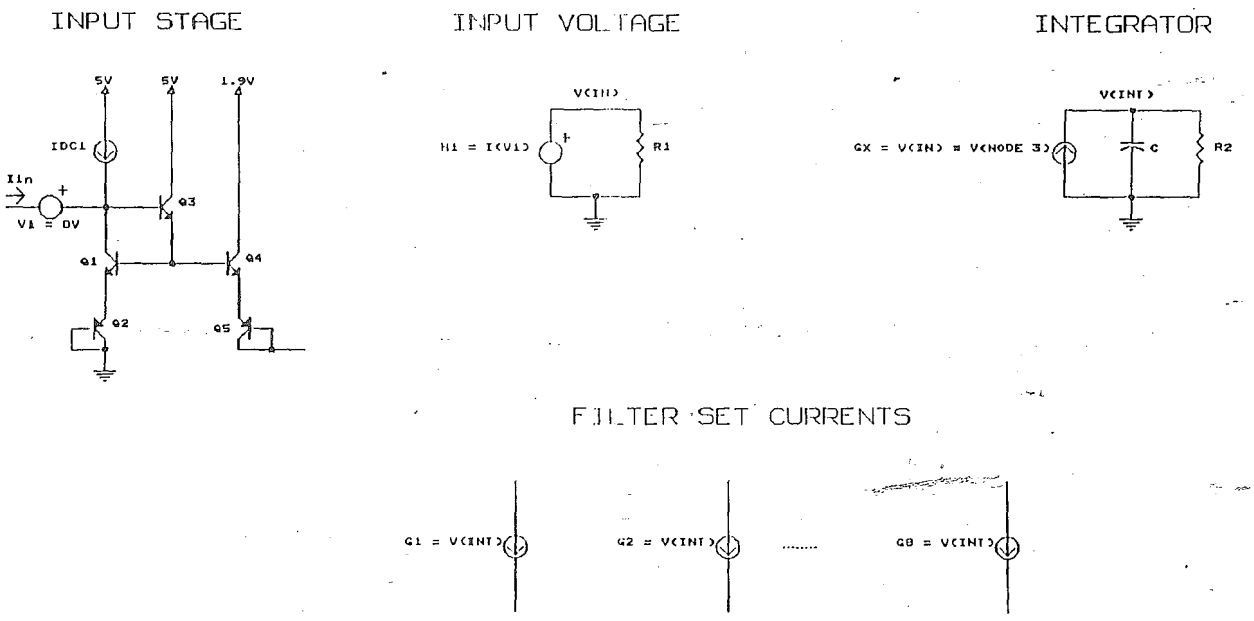

FIG. 24 - ADAPTATION PROCESS

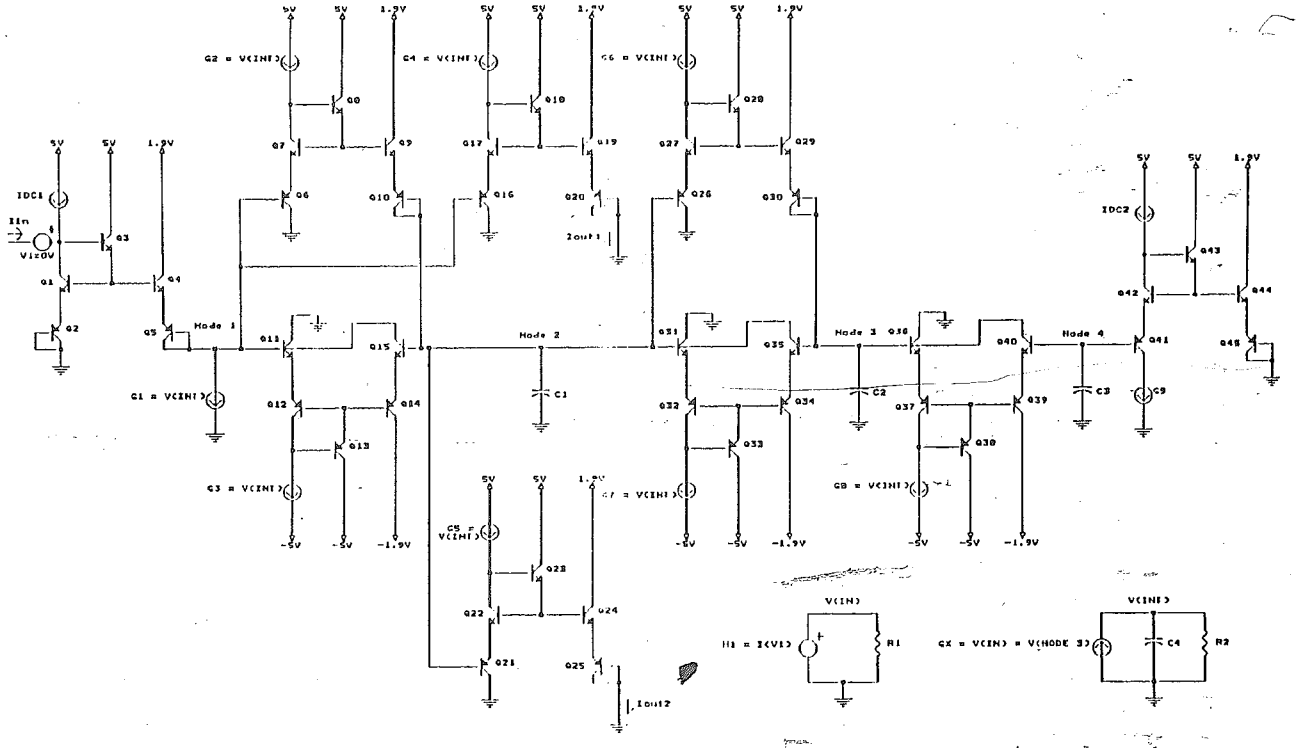

FIG. 25 - ADAPTIVE NOTCH/BANDPASS LOG FILTER

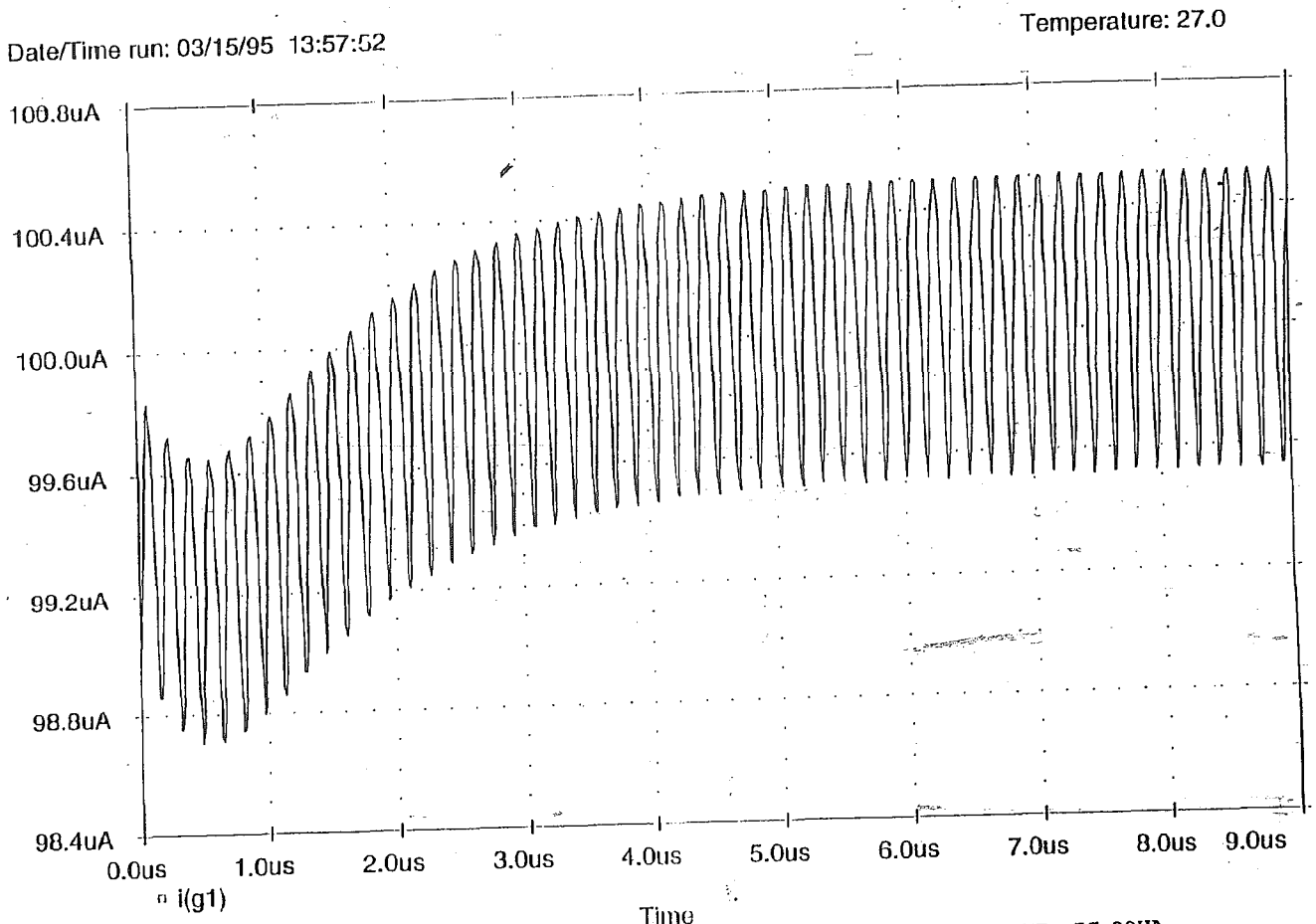

FIG. 26 - ADAPTIVE NOTCH/BANDPASS LOG FILTER, I_0=100UA, C4=10NF, IC=99UA, Q=5, IDEAL MODELS, SET CURRENT ADAPTATION

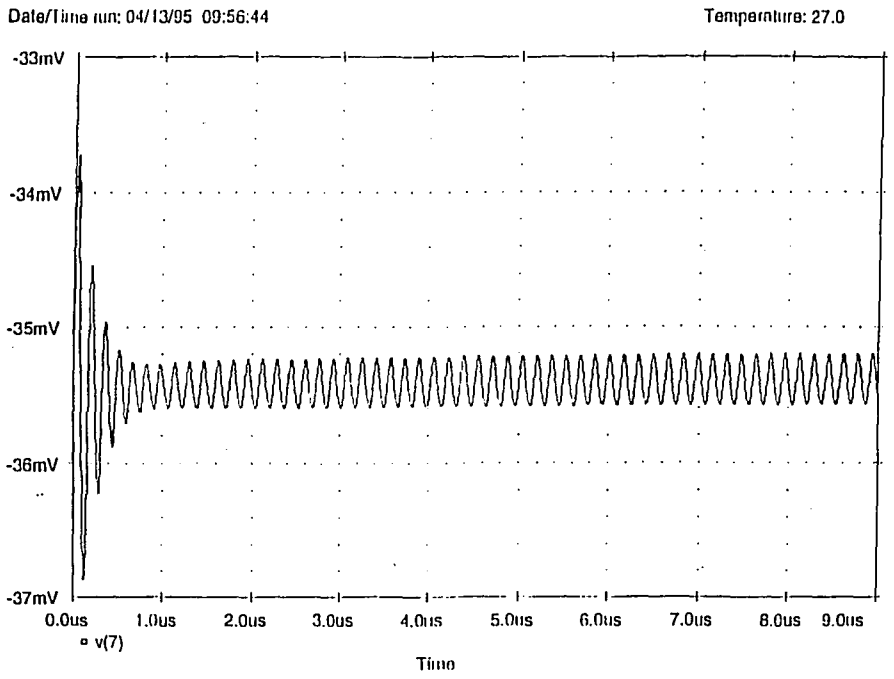

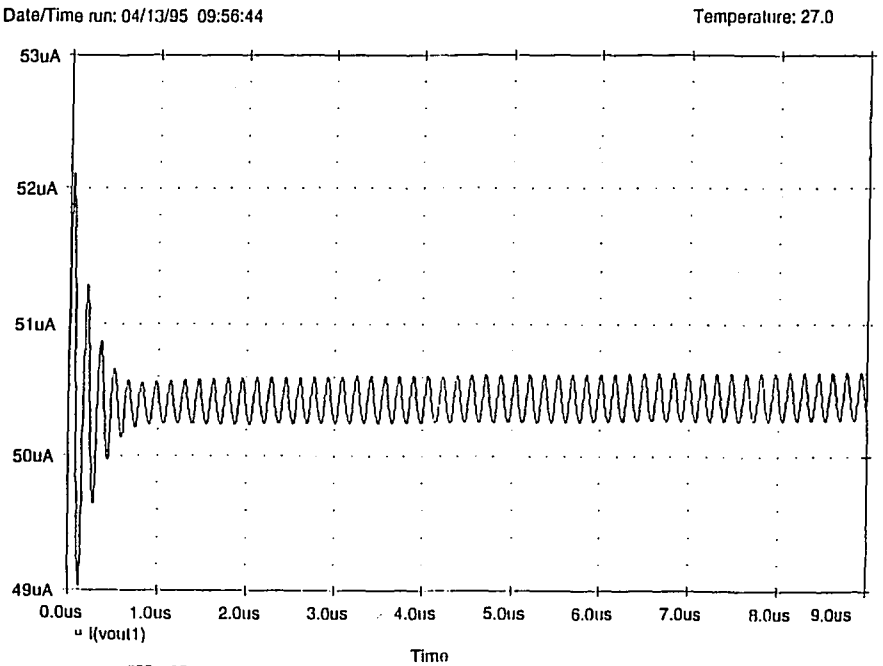

FIG. 27 - ADAPTIVE NOTCH/BANDPASS LOG FILTER, I_o=100UA, C4=10NF, IC=99UA, Q=5, IDEAL MODELS, NOTCH VOLTAGES

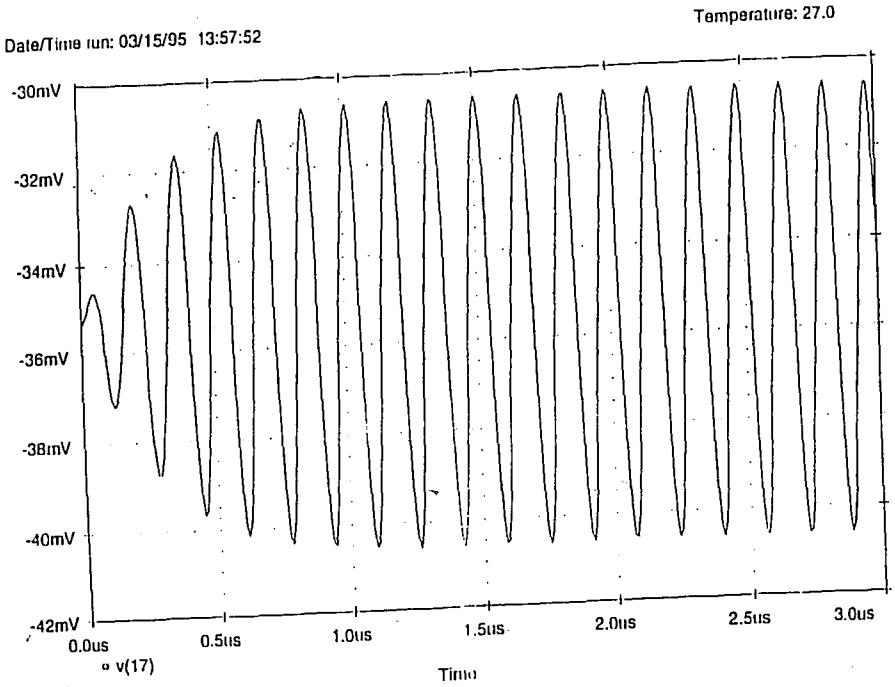

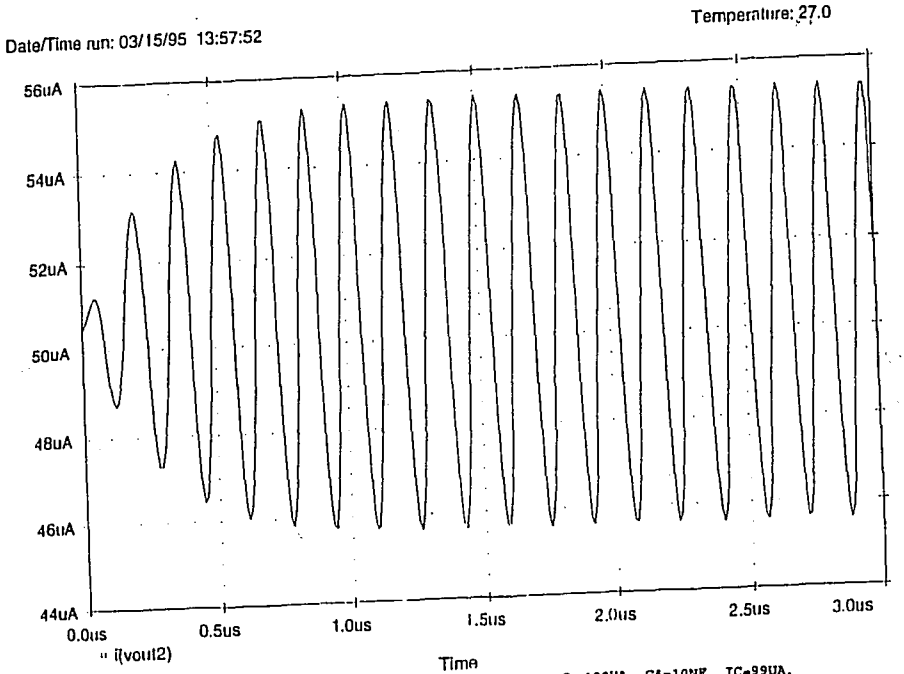

FIG. 28 - ADAPTIVE NOTCH/BANDPASS LOG FILTER, I_0=100UA, C4=10NF, IC=99UA, Q=5, IDEAL MODELS, BANDPASS VOLTAGES

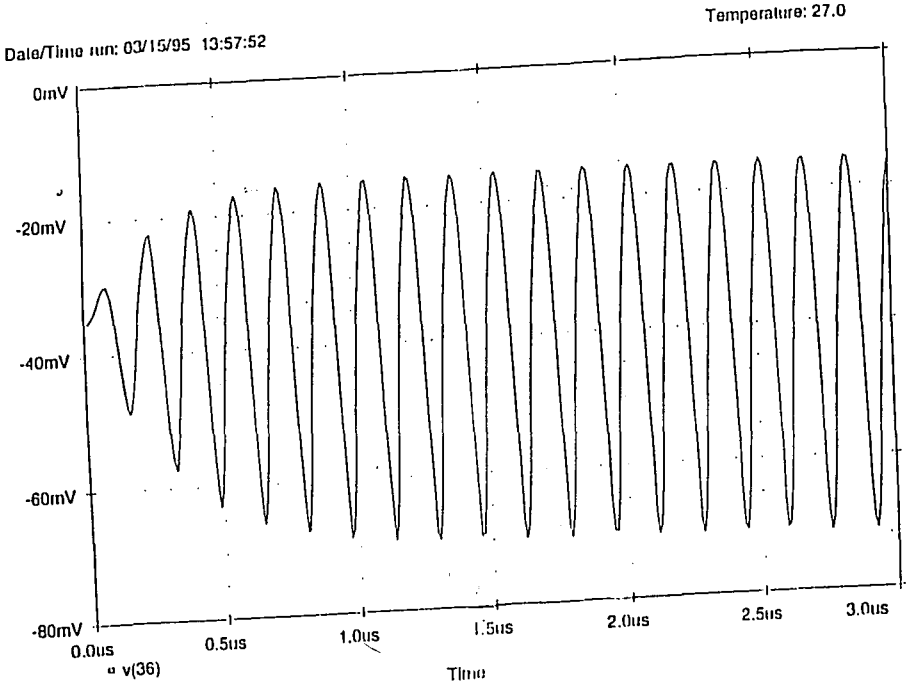

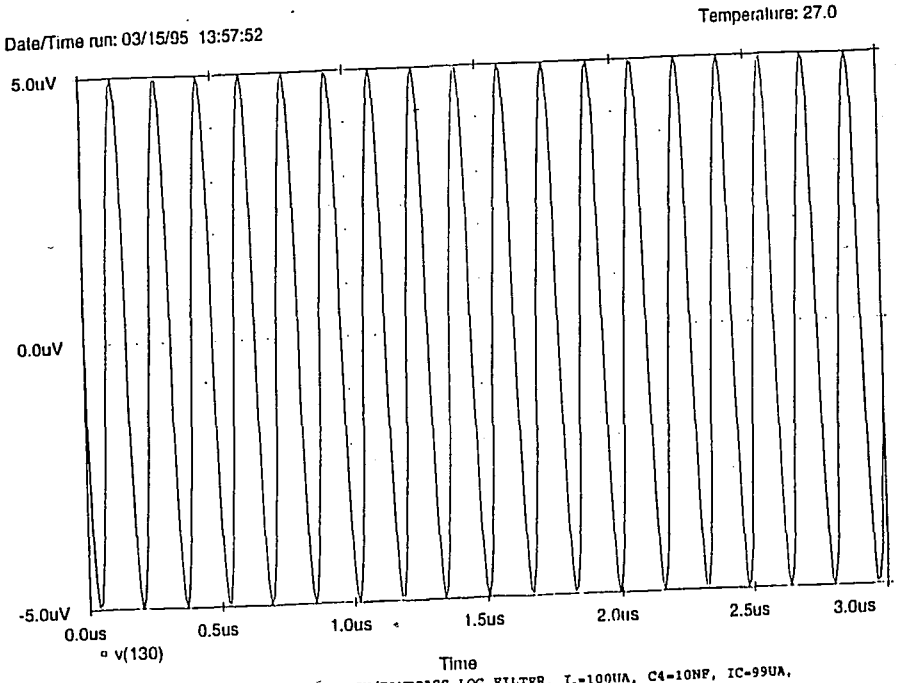

FIG. 29 - ADAPTIVE NOTCH/BANDPASS LOG FILTER, I_0=100UA, C4=10NF, IC=99UA, Q=5, IDEAL MODELS, GRADIENT SIGNAL AND INPUT VOLTAGE

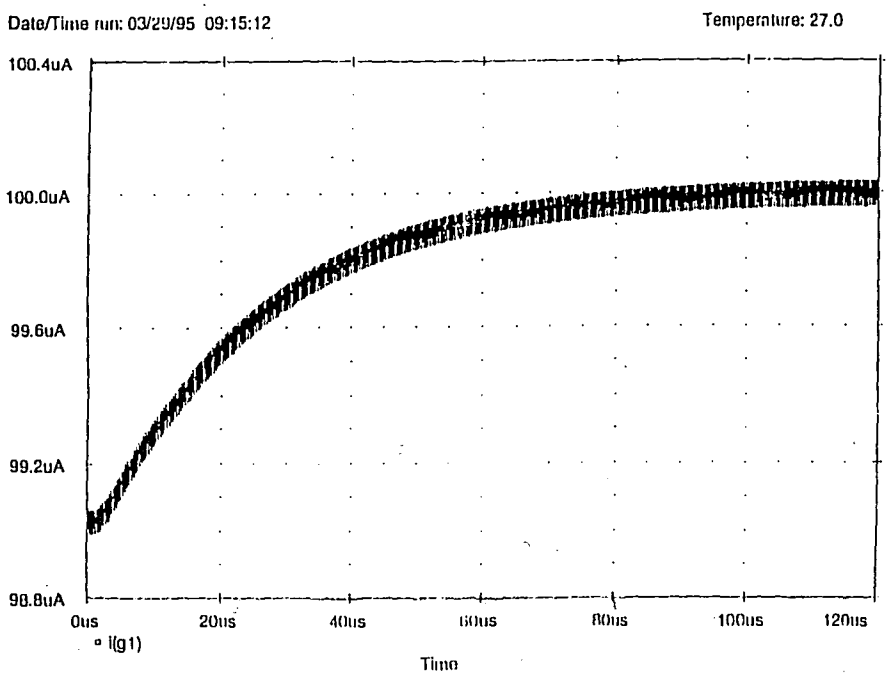

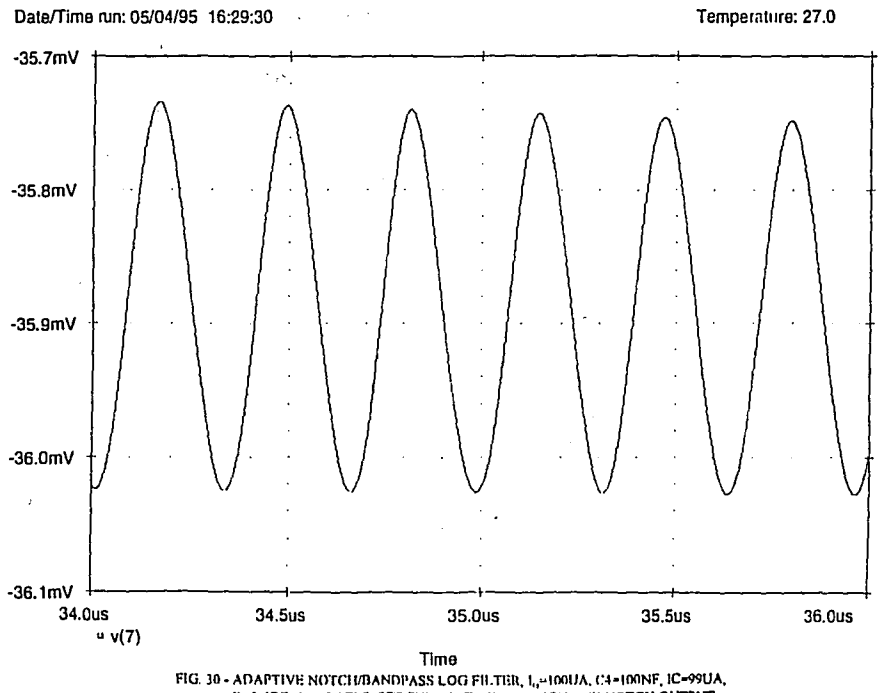

FIG. 30 - ADAPTIVE NOTCH/BANDPASS LOG FILTER, I_0=100UA, C4=100NF, IC=99UA, Q=5, IDEAL MODELS, SET CURRENT ADAPTATION AND NOTCH OUTPUT

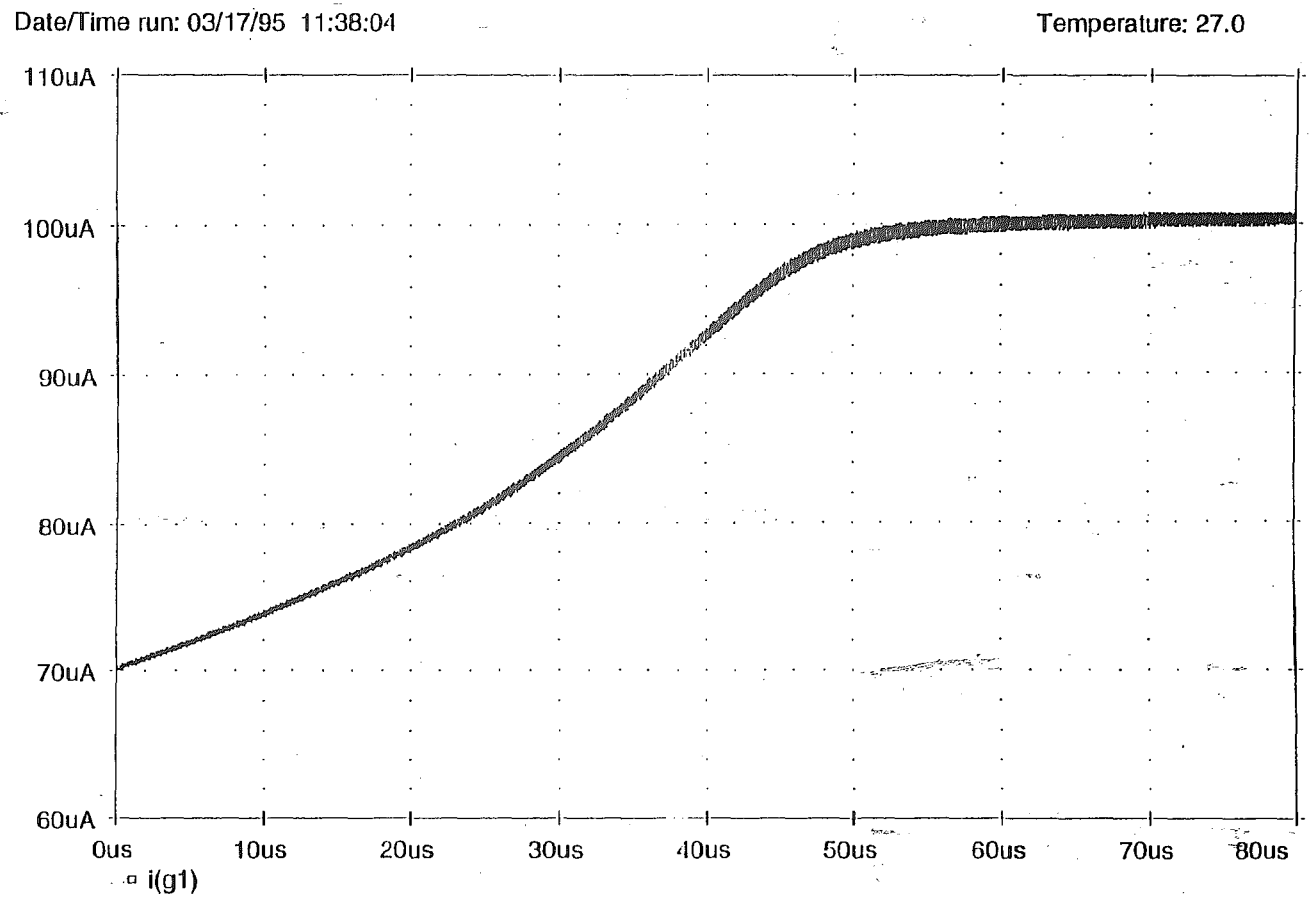

FIG. 31 - ADAPTIVE NOTCH/BANDPASS LOG FILTER, I_0=100UA, C4=5NF, IC=70UA, Q=5, IDEAL MODELS, SET CURRENT ADAPTATION

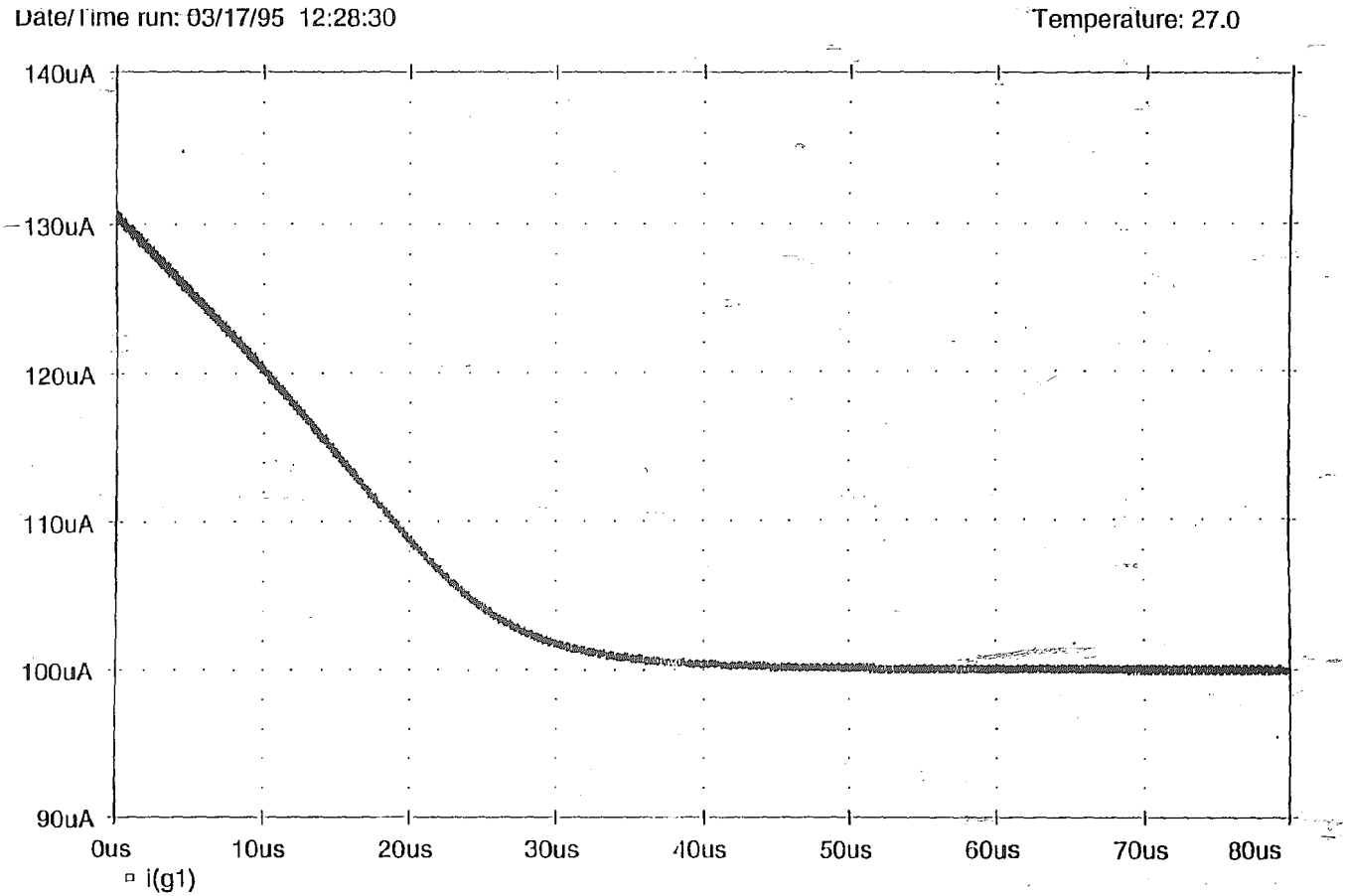

FIG. 32 - ADAPTIVE NOTCH/BANDPASS LOG FILTER, I_0=100UA, C4=5NF, IC=130UA, Q=5, IDEAL MODELS, SET CURRENT ADAPTATION

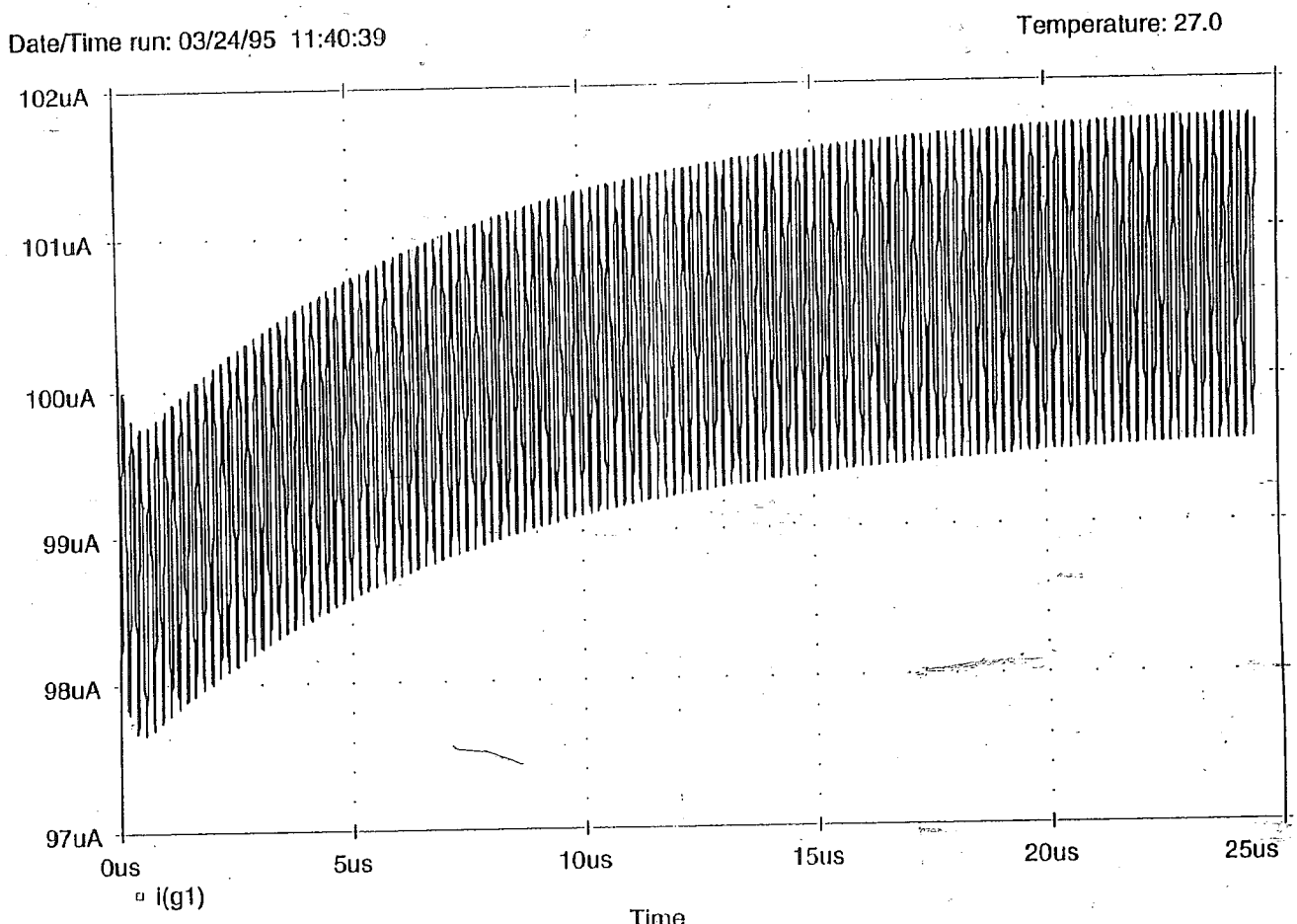

FIG. 33 - ADAPTIVE NOTCH/BANDPASS LOG FILTER, I_0=100UA, C4=2NF, IC=98UA, Q=5, AT&T MODELS, SET CURRENT ADAPTATION

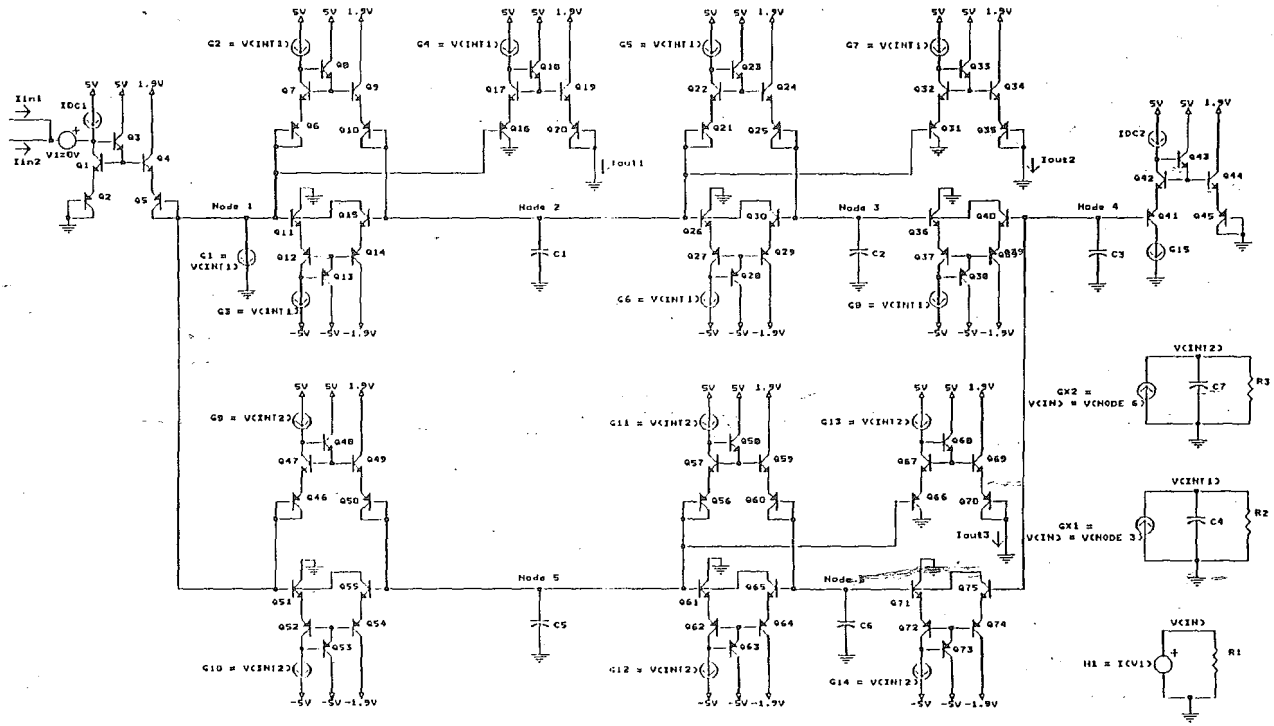

FIG. 34 - ADAPTIVE NOTCH/BANDPASS LOG FILTER, 2 INPUT SINUSOIDS

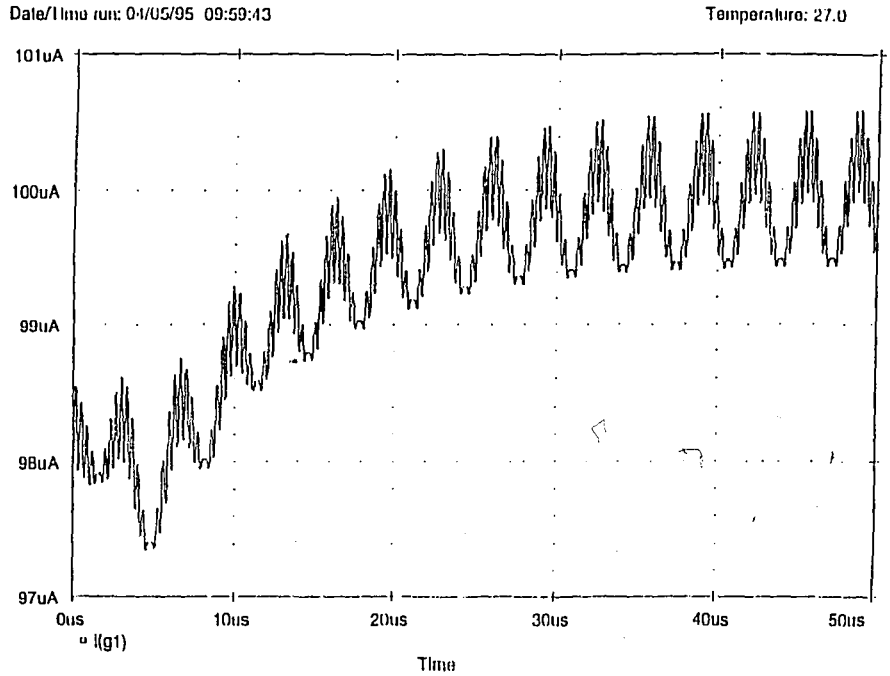

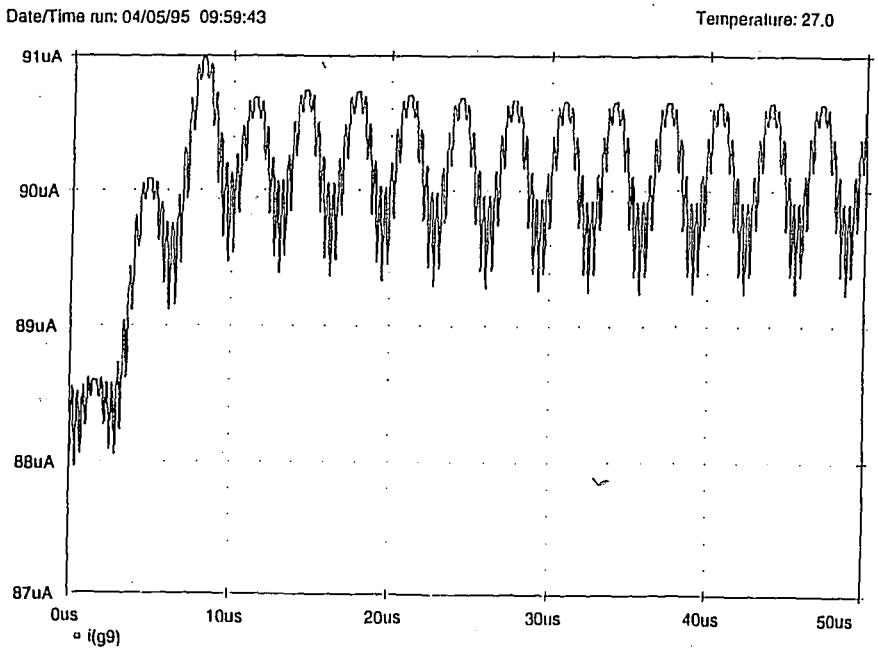

FIG. 35 - ADAPTIVE NOTCH/BANDPASS LOG FILTER, 2 NOTCH BLOCKS, I_{o1}=100UA, I_o2=90UA, C4=C7=40NF, IC1=98UA, IC2=90UA, IDEAL MODELS, SET CURRENTS

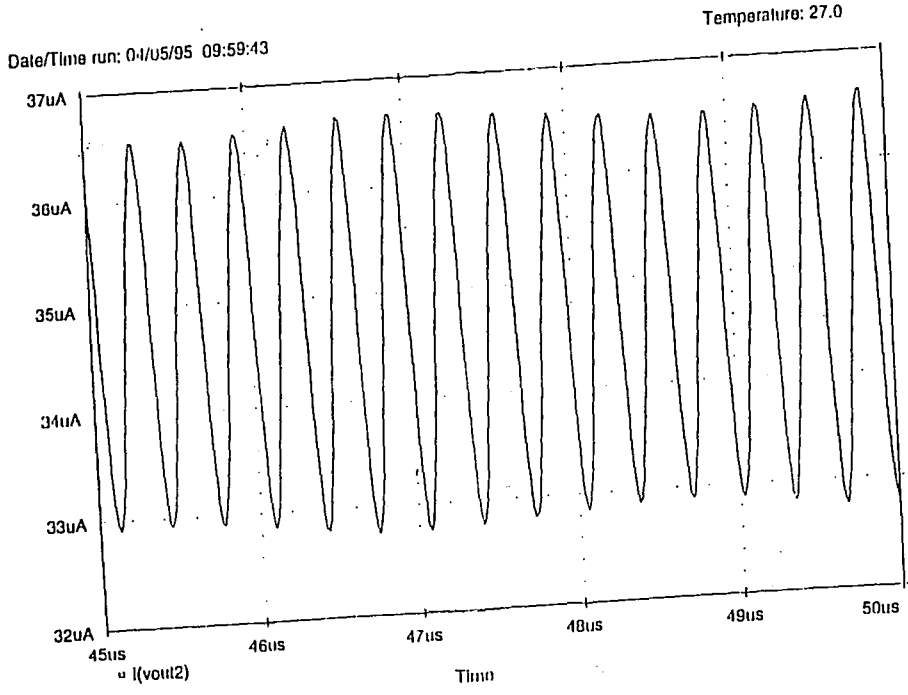

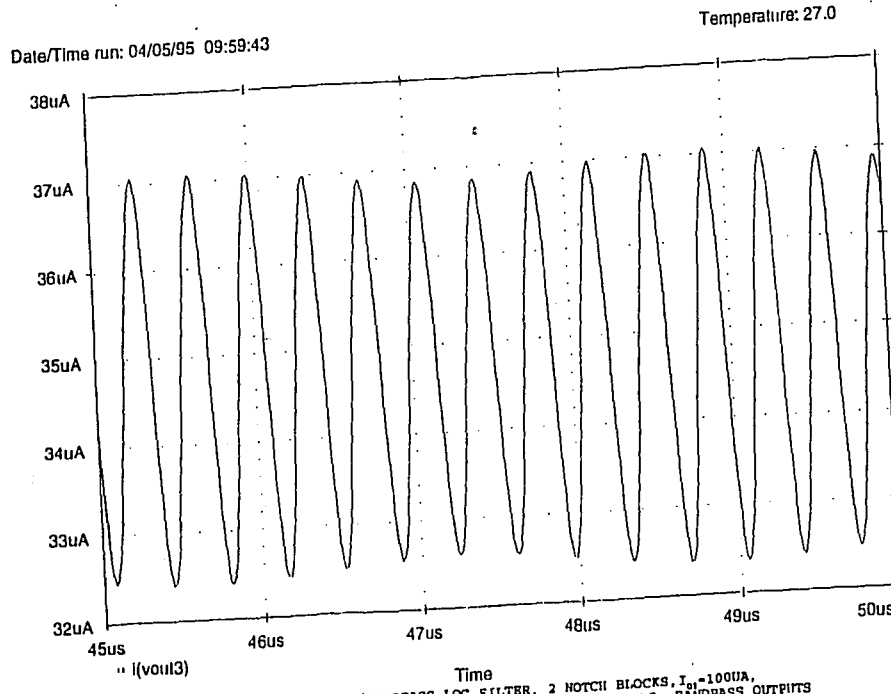

FIG. 36 - ADAPTIVE NOTCH/BANDPASS LOG FILTER, 2 NOTCH BLOCKS, I_{01}=100UA, I_02=90UA, C4=C7=40NF, IC1=98UA, IC2=88UA, IDEAL MODELS, BANDPASS OUTPUTS

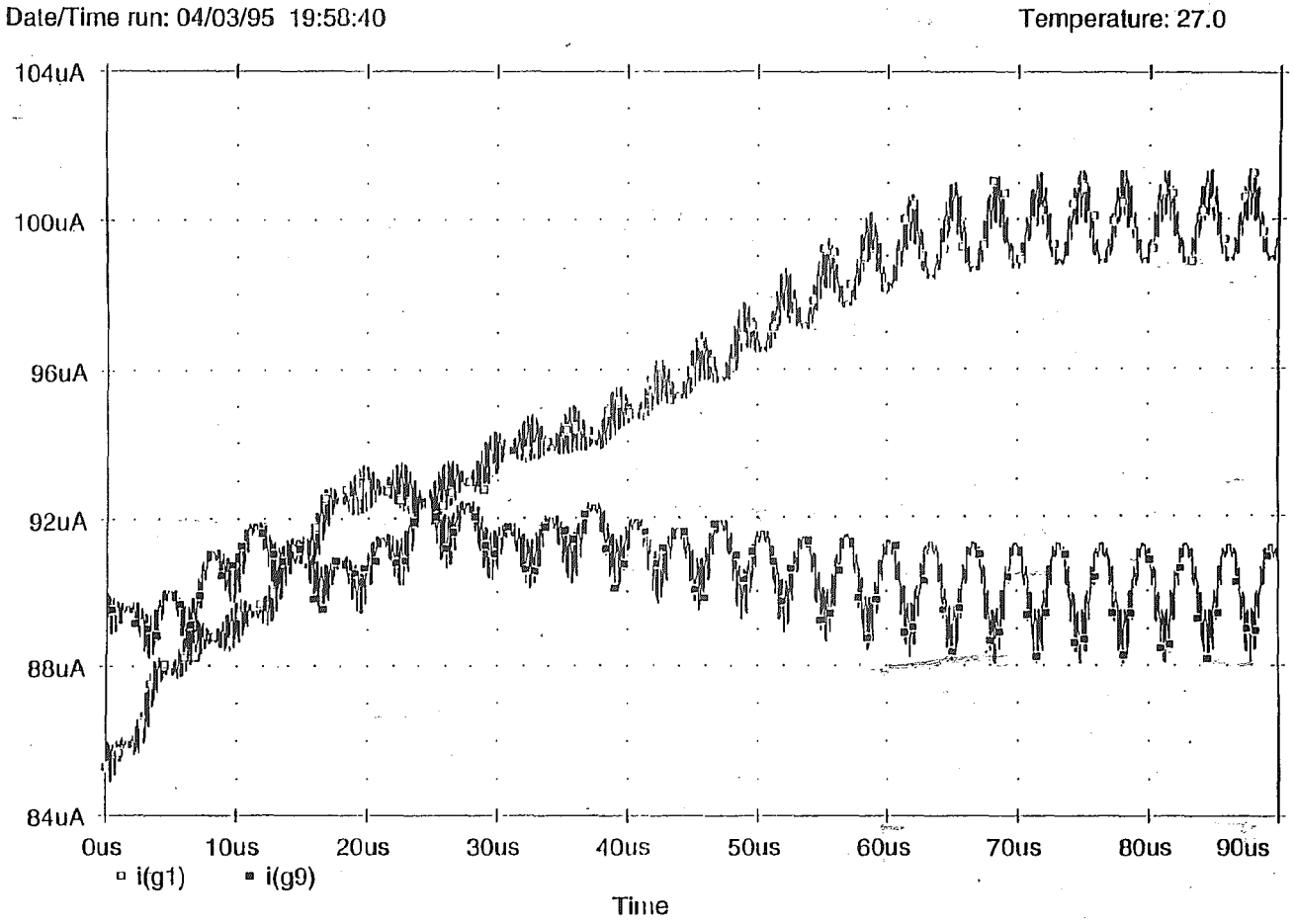

FIG. 37 - ADAPTIVE NOTCH/BANDPASS LOG FILTER, 2 NOTCH BLOCKS, I_{01}=100UA, I_o2=90UA, C4=C7=20NF, IC1=89UA, IC2=85UA, IDEAL MODELS, SET CURRENTS

```
NOTCH/BANDPASS LOG FILTER - Q=8, IO=100UA, IDEAL MODELS
*LUKE STEIGERWALD
V1      1 0 DC 5V
IDC1    1 2 DC 100UA
IIN     0 2 AC 50UA
Q1      1 2 3 14 NX1
Q2      2 3 4 14 NX1
Q3      0 0 4 1 PX1
Q4      5 3 6 14 NX1
V2      5 0 DC 1.9V
Q5      7 7 6 1 PX1
IO1     7 0 DC 100UA
Q6      0 7 8 1 PX1
Q7      10 9 8 14 NX1
IO2     1 10 DC 100UA
Q8      1 10 9 14 NX1
Q9      0 7 11 14 NX1
Q10     13 12 11 1 PX1
IO3     13 14 DC 100UA
V3      0 14 DC 5V
Q11     14 13 12 1 PX1
Q12     15 12 16 1 PX1
V4      0 15 1.9V
Q13     7 17 16 14 NX1
Q14     17 17 18 1 PX1
Q15     5 9 18 14 NX1
C1      17 0 250PF
Q16     0 7 19 1 PX1
Q17     21 20 19 14 NX1
IO4     1 21 DC 100UA
Q18     1 21 20 14 NX1
Q19     5 20 22 14 NX1
Q20     23 0 22 1 PX1
VOUT1   23 0 DC 0
Q21     0 17 24 1 PX1
Q22     26 25 24 14 NX1
IO5     1 26 DC 100UA
Q23     1 26 25 14 NX1
Q24     5 25 27 14 NX1
Q25     28 0 27 1 PX1
VOUT2   28 0 DC 0
Q26     0 17 29 1 PX1
Q27     31 30 29 14 NX1
IO6     1 31 DC 100UA
Q28     1 31 30 14 NX1
Q29     0 17 32 14 NX1
Q30     34 33 32 1 PX1
IO7     34 14 DC 100UA
Q31     14 34 33 1 PX1
Q32     15 33 35 1 PX1
Q33     17 36 35 14 NX1
Q34     36 36 37 1 PX1
Q35     5 30 37 14 NX1
C2      36 0 10PF
Q36     0 36 38 14 NX1
Q37     40 39 38 1 PX1
IO8     40 14 DC 100UA
Q38     14 40 39 1 PX1
Q39     15 39 41 1 PX1
Q40     36 42 41 14 NX1
C3      42 0 500NF
Q41     42 42 43 1 PX1
IO9     42 0 DC 200UA
Q42     5 44 43 14 NX1
Q43     1 45 44 14 NX1
IDC2    1 45 DC 100UA
Q44     45 44 46 14 NX1
Q45     0 0 46 1 PX1
.MODEL NX1 NPN BF=10000
.MODEL PX1 PNP BF=10000
.AC LIN 3000 1MEG 30MEG
.PROBE I(VOUT1) I(VOUT2)
.END
```

APPENDIX B

```
NOTCH/BANDPASS LOG FILTER - Q=5,IO=1UA,AT&T MODELS
*LUKE STEIGERWALD
V1      1 0 DC 5V
IDC1    1 2 DC 100UA
IIN     0 2 AC 50UA
Q1      1 2 3 14 NX1
Q2      2 3 4 14 NX1
Q3      0 0 4 1 PX1
Q4      5 3 6 14 NX1
V2      5 0 DC 1.9V
Q5      7 7 6 1 PX1
IO1     7 0 DC 1UA
Q6      0 7 8 1 PX1
Q7      10 9 8 14 NX1
IO2     1 10 DC 1UA
Q8      1 10 9 14 NX1
Q9      0 7 11 14 NX1
Q10     13 12 11 1 PX1
IO3     13 14 DC 1UA
V3      0 14 DC 5V
Q11     14 13 12 1 PX1
Q12     15 12 16 1 PX1
V4      0 15 1.9V
Q13     7 17 16 14 NX1
Q14     17 17 18 1 PX1
Q15     5 9 18 14 NX1
INR     1 17 933NA
C1      17 0 250PF
Q16     0 7 19 1 PX1
Q17     21 20 19 14 NX1
IO4     1 21 DC 1UA
Q18     1 21 20 14 NX1
Q19     5 20 22 14 NX1
Q20     23 0 22 1 PX1
VOUT1   23 0 DC 0
Q21     0 17 24 1 PX1
Q22     26 25 24 14 NX1
IO5     1 26 DC 1UA
Q23     1 26 25 14 NX1
Q24     5 25 27 14 NX1
Q25     28 0 27 1 PX1
VOUT2   28 0 DC 0
Q26     0 17 29 1 PX1
Q27     31 30 29 14 NX1
IO6     1 31 DC 1UA
Q28     1 31 30 14 NX1
Q29     0 17 32 14 NX1
Q30     34 33 32 1 PX1
IO7     34 14 DC 1UA
Q31     14 34 33 1 PX1
Q32     15 33 35 1 PX1
Q33     17 36 35 14 NX1
Q34     36 36 37 1 PX1
Q35     5 30 37 14 NX1
C2      36 0 10PF
Q36     0 36 38 14 NX1
Q37     40 39 38 1 PX1
IO8     40 14 DC 1UA
Q38     14 40 39 1 PX1
Q39     15 39 41 1 PX1
Q40     36 42 41 14 NX1
C3      42 0 500NF
Q41     42 42 43 1 PX1
IO9     42 0 DC 2UA
Q42     5 44 43 14 NX1
Q43     1 45 44 14 NX1
IDC2    1 45 DC 100UA
Q44     45 44 46 14 NX1
Q45     0 0 46 1 PX1
.MODEL NX1 NPN RB=524.6 IRB=0 RBM=25 RC=50 RE=1 IS=121E-18 EG=1.206 XTI=2
+ XTB=1.538 BF=137.5 IKF=6.974E-3 NF=1 VAF=159.4 ISE=36E-16 NE=1.713 BR=0.7258
+ IKR=2.198E-3 NR=1 VAR=10.73 ISC=0 NC=2 TF=0.425E-9 TR=0.425E-8 CJE=0.214E-12
+ VJE=0.5 MJE=0.28 CJC=0.983E-13 VJC=0.5 MJC=0.3 XCJC=0.034 CJS=0.913E-12
+ VJS=0.64 MJS=0.4 FC=0.5
.MODEL PX1 PNP RB=327 IRB=0 RBM=24.55 RC=50 RE=3 IS=73.5E-18 EG=1.206 XTI=1.7
```

```
+ XTB=1.866 BF=110.0 IKF=2.359E-3 NF=1 VAF=51.8 ISE=25.1E-16 NE=1.650 BR=0.4745
+ IKR=6.478E-3 NR=1 VAR=9.96 ISC=0 NC=2 TF=0.610E-9 TR=0.610E-8 CJE=0.180E-12
+ VJE=0.5 MJE=0.28 CJC=0.164E-12 VJC=0.8 MJC=0.4 XCJC=0.037 CJS=1.03E-12 VJS=0.55
+ MJS=0.35 FC=0.5
.AC LIN 8000 10K 300K
.PROBE V(7) I(VOUT1) I(VOUT2) V(17)
.END
```

```
ADAPTIVE NOTCH/BANDPASS LOG FILTER - IO=100UA,C4=10NF,IC=99UA,Q=5,IDEAL MODELS
*LUKE STEIGERWALD
V1      1 0 DC 5V
IDC1    1 2 DC 100UA
IIN     0 120 SIN(0 5UA 6.152866MEG)
VT3     2 120 DC 0
Q1      1 2 3 14 NX1
Q2      2 3 4 14 NX1
Q3      0 0 4 1 PX1
Q4      5 3 6 14 NX1
V2      5 0 DC 1.9V
Q5      7 7 6 1 PX1
G1      7 100 200 0 1
VT1     100 0 DC 0
Q6      0 7 8 1 PX1
Q7      10 9 8 14 NX1
G2      1 10 200 0 1
Q8      1 10 9 14 NX1
Q9      0 7 11 14 NX1
Q10     13 12 11 1 PX1
G3      13 14 200 0 1
V3      0 14 DC 5V
Q11     14 13 12 1 PX1
Q12     102 12 16 1 PX1
VT2     102 15 DC 0
V4      0 15 DC 1.9V
Q13     7 17 16 14 NX1
Q14     17 17 18 1 PX1
Q15     5 9 18 14 NX1
C1      17 0 250PF
Q16     0 7 19 1 PX1
Q17     21 20 19 14 NX1
IO4     1 21 DC 100UA
Q18     1 21 20 14 NX1
Q19     5 20 22 14 NX1
Q20     23 0 22 1 PX1
VOUT1   23 0 DC 0
Q21     0 17 24 1 PX1
Q22     26 25 24 14 NX1
IO5     1 26 DC 100UA
Q23     1 26 25 14 NX1
Q24     5 25 27 14 NX1
Q25     28 0 27 1 PX1
VOUT2   28 0 DC 0
Q26     0 17 29 1 PX1
Q27     31 30 29 14 NX1
G6      1 31 200 0 1
Q28     1 31 30 14 NX1
Q29     0 17 32 14 NX1
Q30     34 33 32 1 PX1
G7      34 14 200 0 1
Q31     14 34 33 1 PX1
Q32     15 33 35 1 PX1
Q33     17 36 35 14 NX1
Q34     36 36 37 1 PX1
Q35     5 30 37 14 NX1
C2      36 0 10PF
Q36     0 36 38 14 NX1
Q37     40 39 38 1 PX1
G8      40 14 200 0 1
Q38     14 40 39 1 PX1
Q39     15 39 41 1 PX1
Q40     36 42 41 14 NX1
C3      42 0 500NF
Q41     42 42 43 1 PX1
F1      42 0 POLY(2) VT1 VT2 0 1 1
Q42     5 44 43 14 NX1
Q43     1 45 44 14 NX1
IDC2    1 45 DC 100UA
Q44     45 44 46 14 NX1
Q45     0 0 46 1 PX1
H1      130 0 VT3 1
R1      130 0 10K
GX      0 200 POLY(2) (130,0) (36,0) 0 0 0 0 1
C4      200 0 10NF
```

```
R2      200 0 100MEG
.IC V(200)=99UV
.MODEL NX1 NPN BF=10000
.MODEL PX1 PNP BF=10000
.TRAN 8.68NS 9US 0 8.68NS
.OPTIONS ITL5=0
.PROBE I(G1) I(VOUT1) I(VOUT2) V(7) V(17) V(36) V(130)
.END
```

VITA

The author was born in Syracuse, NY on April 30, 1970 to Francis and Patricia Steigerwald. He attended Cazenovia Central High School in Cazenovia, NY and graduated from the University of Pennsylvania in Philadelphia, PA in May, 1992 with a Bachelor of Science degree in electrical engineering. Before attending Lehigh University he worked for United Technologies Automotive, Inc. in Dearborn, MI where he was awarded the patent "Power Distribution Box and System."

END OF TITLE